Computer Assisted Proof of Drift Orbits Along Normally Hyperbolic Manifolds II: Application to the Restricted Three Body Problem

Maciej J. Capiński[a,1], Natalia Wodka[a,1,*]

[a] *Faculty of Applied Mathematics, AGH University of Science and Technology, al. Mickiewicza 30, 30-059 Kraków, Poland.*

Abstract

We present a computer assisted proof or diffusion in the Planar Elliptic Restricted Three Body Problem. We treat the elliptic problem as a perturbation of the circular problem, where the perturbation parameter is the eccentricity of the primaries. The unperturbed system preserves energy, and we show that for sufficiently small perturbations we have orbits with explicit energy changes, independent from the size of the perturbation. The result is based on shadowing of orbits along transversal intersections of stable/unstable manifolds of a normally hyperbolic cylinder.

Keywords: Normally hyperbolic manifold, Arnold diffusion, scattering map, topological shadowing, computer assisted proof, three body problem
2010 MSC: 37J25, 37J40

1. Introduction

Autonomous Hamiltonian systems have an integral of motion given by the Hamiltonian. We shall refer to this integral as the energy. Our question is whether for an arbitrarily small perturbation we can have orbits, which change in energy by a prescribed constant independent form the size of the perturbation.

In our case, the system of interest is the Planar Restricted Three Body Problem that describes the motion of a small massless particle under the gravitational pull of two large bodies. They rotate on Keplerian orbits and we call them primaries. The motion of the massless particle is on the same plane as the primaries. When the Keplerian orbit is circular, then in the coordinate frame which rotates with the primaries we have an autonomous Hamiltonian system; the Planar Circular Restricted Three Body Problem (PCR3BP). When the Keplerian orbits are elliptic, then we deal with the Elliptic Problem (PER3BP), which is a time dependent Hamiltonian system.

The system we study has a normally hyperbolic invariant manifold (NHIM) prior to the perturbation, with stable and unstable manifolds which intersect transversally. This means that we consider an 'apriori-chaotic' system. (This is a much simpler problem than starting with a fully integrable system; as in the famous example of Arnold [1].) Our diffusion mechanism is

*Corresponding author.
[1] Partially supported by the NCN grant 2018/29/B/ST1/00109.

based on establishing the existence of trajectories that shadow the intersections of the stable and unstable manifolds and change energy under the influence of the perturbation.

Our result is based on the geometric and shadowing results of Delshams, Gidea, de la Llave and Seara. At the core of the mechanism is the scattering map [2]; that is a map which for a point on the NHIM assigns another point from the NHIM, if their unstable and stable fibres intersect in a nontrivial way. The benefit of studying a scattering map is twofold. Firstly, one can exploit perturbative techniques to study the effect of the parameter on the scattering map. This is typically done by using Melnikov integrals in the case of continuous systems, or Melnikov sums in the case of discrete systems [2, 3]. Once the effects of the perturbation on the scattering map is established, the second benefit is that there exist true orbits of the system, which will shadow the 'pseudo orbits' of the scattering map [4]. This means that if one can prove existence of 'pseudo orbits' of the scattering map which have macroscopic changes in energy, then this ensures the existence of true trajectories of the system that will do the same.

The strategy for proving diffusion using this scheme is described in [2, 3, 4, 5]. For our proof we will use the results from [6], which provides a formulation for these methods, that can be implemented to obtain a computer assisted proof. The main feature of [6] is that the assumptions needed for the diffusion mechanism can be validated in a finite number of steps by checking various bounds on the properties of the system.

In our case the components that need to be established are the following. We establish bounds on the family of Lyapunov orbits in the PCR3BP, which constitute our NHIM prior to the perturbation. Next we establish bounds for the local stable/unstable manifolds of the NHIM, and prove that they intersect transversally. We ensure that the scattering map is well defined and obtain explicit bounds on its dynamics. We also validate twist conditions, which ensure that the NHIM after perturbation contains a Cantor set of KAM tori. Then we can apply the theorems from [6] to prove diffusion. All the above steps can be established with the assistance of rigorous, interval arithmetic based estimates, performed with the aid of a computer.

For proofs of diffusion in the PER3BP a computer assisted approach is not strictly necessary. The paper [7] provides an analytic proof of diffusion in the PER3BP. This result also used the scattering map theory and shadowing as the mechanism. To obtain the analytic proof though [7] required that the mass of one of the primaries is sufficiently small, and that the angular momentum of the massless particle is sufficiently large. The difference with the result from the current paper is that we can work with the explicit mass of Jupiter and with the explicit energy of a massless particle, which corresponds to that of the comet Oterma. As in [7] we have to assume that the eccentricity of the system is sufficiently small.

A recent result which works with explicit masses, explicit energy and explicit interval of eccentricities that starts from zero and reaches a physical value is given in [8]. This is based on a computer assisted construction of 'correctly aligned windows'. The difference is that in the current paper we only need to establish the intersections of the manifolds for the unperturbed system, and check some explicit conditions from [6]. The shadowing of orbits is then automatically taken care of by [4], and we do not need to carry out the explicit construction of windows as in [8]. Our results are weaker though than [8].

The geometric setup for our method follows very closely that from [9, 10]. There are some small differences though, the main being that we use Poincaré maps and compute finite Melnikov sums, instead of Melnikov integrals. Our original plan was to follow directly the setup from [10], but we have found that computing sharp bounds on integrals along trajectories is more difficult than computing bounds on sums along discrete trajectories of Poincaré maps.

Our tool for the computer assisted implementation is the CAPD[2] library [11]. The tools which we use are quite standard: The existence of the family of Lyapunov orbits as well as the proof of their homoclinic orbits is done by exploiting symmetry properties of the PCR3BP, combined with parallel shooting and the Krawczyk method. To establish bounds on the stable and unstable manifolds and the transversality of their intersections needed to ensure that the scattering map is well defined we use cones. The assumptions of theorems [6] leading to diffusion can then be checked by computing sums along finite fragments of homoclinic orbits.

The paper is organised as follows. Section 2 contains preliminaries, which include the Krawczyk method, introduction to the scattering map and the shadowing results for scattering maps, as well as a short introduction to the restricted three body problem. In section 3 we state the main result of the paper, which is written in Theorem 12. Section 4 contains the proof of the main theorem. Some of the technical issues are delegated to the Appendix.

2. Preliminaries

2.1. Notations

For a set U in a topological space we will denote its interior by $\mathrm{int}U$, its closure by $\bar{U}$ and its boundary by ∂U.

We shall denote identity by Id. For a point p expressed in some coordinates $p = (x, y)$ we shall denote by π_x and π_y the projections onto the given coordinates, i.e. $\pi_x p = x$ and $\pi_y p = y$. For $p = (p_1, \ldots, p_n)$ we will write π_i to denote the projection onto the i-th coordinate, i.e. $\pi_i p = p_i$.

We write $\|\cdot\|_{\max}$ for the maximum norm in $\mathbb{R}^n$, and for a matrix A write $\|A\|_{\max}$ for the matrix norm induced by $\|\cdot\|_{\max}$.

We shall denote a k-dimensional torus as $\mathbb{T}^k$, with the convention that $\mathbb{T} := \mathbb{R} \bmod 2\pi$.

2.2. Krawczyk method

We refer to a cartesian product of intervals as an interval set. For a set $U \subset \mathbb{R}^n$ we shall denote by $[U]$ an interval set such that $U \subset [U]$. We refer to such set as an interval enclosure of U. An interval enclosure is not unique. In our applications we shall consider interval enclosures of objects of interest; namely: fixed points, periodic orbits, homoclinic orbits and invariant manifolds. The smaller the interval enclosure is, the more accurate is our bound on the object of interest. We shall refer to a matrix whose coefficients are intervals as an interval matrix.

For a C^1 function $F : \mathbb{R}^n \to \mathbb{R}^n$ we denote by $[DF(X)] \subset \mathbb{R}^{n\times n}$ the interval matrix enclosure of the derivatives of F on X, namely we consider

$$[DF(X)] = \left\{ A = \left(a_{i,j}\right) : a_{ij} \in \left[\inf_{x\in X} \frac{\partial f_i}{\partial x_j}(x), \sup_{x\in X} \frac{\partial f_i}{\partial x_j}(x) \right] \right\}.$$

Below theorem, known as the Krawczyk method, can be used to establish bounds on zeros of functions.

Theorem 1. *[12]Let $F : \mathbb{R}^n \to \mathbb{R}^n$ be a C^1 function. Let $X \subset \mathbb{R}^n$ be an interval set, let $x \in X$, let $C \in \mathbb{R}^{n\times n}$ be a linear isomorphism and let*

$$K(x, X, F) := x - CF(x) + (Id - C[DF(X)])(X - x).$$

[2]Computer Assisted Proofs in Dynamics: http://capd.ii.uj.edu.pl

If

$$K(x, X, F) \subset \text{int}X,$$

then there exists a unique point $x^* \in X$ for which

$$F(x^*) = 0.$$

2.3. Normally hyperbolic invariant manifolds and the scattering map

In this section we recall the results which we use for our diffusion mechanism. We follow the setup from [6], which is based on the scattering map theory described in [2], and the diffusion mechanism from [4], which is the main tool for our proof.

Definition 2. *Let M be a smooth n-dimensional manifold, and let $f : M \to M$ be a C^r diffeomorphism, with $r > 1$. Let $\Lambda \subset M$ be a compact manifold without boundary, invariant under f, i.e., $f(\Lambda) = \Lambda$. We say that Λ is a normally hyperbolic invariant manifold (with symmetric rates) if there exists a constant $C > 0$, rates $0 < \lambda < \mu^{-1} < 1$ and a Tf-invariant splitting for every $x \in \Lambda$*

$$T_xM = E^u_x \oplus E^s_x \oplus T_x\Lambda$$

such that

$$v \in E^u_x \Leftrightarrow \left\|Df^k(x)v\right\| \leq C\lambda^{-k}\|v\|, \quad k \leq 0, \tag{1}$$

$$v \in E^s_x \Leftrightarrow \left\|Df^k(x)v\right\| \leq C\lambda^{k}\|v\|, \quad k \geq 0, \tag{2}$$

$$v \in T_x\Lambda \Rightarrow \left\|Df^k(x)v\right\| \leq C\mu^{|k|}\|v\|, \quad k \in \mathbb{Z}. \tag{3}$$

Let $d(x, \Lambda)$ stand for the distance between a point x and the manifold Λ. Given a normally hyperbolic invariant manifold and a suitable small tubular neighbourhood $U \subset M$ of Λ one defines its local unstable and local stable manifold [13] as

$$W^u_\Lambda(f, U) = \left\{y \in M \,|\, f^k(y) \in U, d\left(f^k(y), \Lambda\right) \leq C_y\lambda^{|k|},\, k \leq 0\right\},$$
$$W^s_\Lambda(f, U) = \left\{y \in M \,|\, f^k(y) \in U, d\left(f^k(y), \Lambda\right) \leq C_y\lambda^{k},\, k \geq 0\right\},$$

where C_y is a positive constant, which can depend on y. We define the (global) unstable and stable manifolds as

$$W^u_\Lambda(f) = \bigcup_{n\geq 0} f^n\left(W^u_\Lambda(f, U)\right), \qquad W^s_\Lambda(f) = \bigcup_{n\geq 0} f^{-n}\left(W^s_\Lambda(f, U)\right).$$

The manifolds $W^u_\Lambda(f, U)$, $W^s_\Lambda(f, U)$, $W^u_\Lambda(f)$ and $W^s_\Lambda(f)$ are foliated by

$$W^u_x(f, U) = \left\{y \in M \,|\, f^k(y) \in U, d(f^k(y), f^k(x)) \leq C_{x,y}\lambda^{|k|},\, k \leq 0\right\},$$
$$W^s_x(f, U) = \left\{y \in M \,|\, f^k(y) \in U, d(f^k(y), f^k(x)) \leq C_{x,y}\lambda^{k},\, k \geq 0\right\},$$

where $x \in \Lambda$ and $C_{x,y}$ is a positive constant, which can depend on x and y,

$$W^u_x(f) = \bigcup_{n\geq 0} f^n\left(W^u_{f^{-n}(x)}(f, U)\right), \qquad W^s_x(f) = \bigcup_{n\geq 0} f^{-n}\left(W^s_{f^n(x)}(f, U)\right).$$

Let

$$l < \min\left\{r, \frac{|\log\lambda|}{\log\mu}\right\}. \tag{4}$$

The manifold Λ is C^l smooth, the manifolds $W^u_\Lambda(f), W^s_\Lambda(f)$ are C^{l-1} and $W^u_x(f)$, $W^s_x(f)$ are C^r [2]. Normally hyperbolic manifolds, as well as their stable and unstable manifolds and their fibres persist under small perturbations [13].

From now let (M,ω) be a smooth symplectic manifold. Let us assume that $\Lambda \subset M$ is a normally hyperbolic invariant manifold for a C^r symplectic map $f : M \to M$, where $r > 1$. We assume that Λ is even dimensional and symplectic with the symplectic form $\omega|_\Lambda$, and that $f|_\Lambda$ is symplectic on Λ. We define two maps,

$$\Omega_+ : W^s_\Lambda(f) \to \Lambda,$$
$$\Omega_- : W^u_\Lambda(f) \to \Lambda,$$

where $\Omega_+(x) = x_+$ iff $x \in W^s_{x_+}(f)$, and $\Omega_-(x) = x_-$ iff $x \in W^u_{x_-}(f)$. These are referred to as the wave maps.

Definition 3. *We say that a manifold $\Gamma \subset W^u_\Lambda(f) \cap W^s_\Lambda(f)$ is a homoclinic channel for Λ if the following conditions hold:*

(i) for every $x \in \Gamma$

$$T_x W^s_\Lambda(f) + T_x W^u_\Lambda(f) = T_x M, \tag{5}$$
$$T_x W^s_\Lambda(f) \cap T_x W^u_\Lambda(f) = T_x \Gamma, \tag{6}$$

(ii) the fibres of Λ intersect Γ transversally in the following sense

$$T_x\Gamma \oplus T_x W^s_{x_+}(f) = T_x W^s_\Lambda(f), \tag{7}$$
$$T_x\Gamma \oplus T_x W^u_{x_-}(f) = T_x W^u_\Lambda(f), \tag{8}$$

for every $x \in \Gamma$,

(iii) the wave maps $(\Omega_\pm)|_\Gamma : \Gamma \to \Lambda$ are diffeomorphisms onto their image.

Definition 4. *Assume that Γ is a homoclinic channel for Λ and let*

$$\Omega^\Gamma_\pm := (\Omega_\pm)|_\Gamma.$$

We define a scattering map σ^Γ for the homoclinic channel Γ as

$$\sigma^\Gamma := \Omega^\Gamma_+ \circ \left(\Omega^\Gamma_-\right)^{-1} : \Omega^\Gamma_-(\Gamma) \to \Omega^\Gamma_+(\Gamma).$$

We have the following theorem, which is the basis for the diffusion mechanism from the subsequent section.

Theorem 5. *[4] Assume that $f : M \to M$ is a sufficiently smooth map, $\Lambda \subset M$ is a normally hyperbolic invariant manifold with stable and unstable manifolds which intersect transversally along a homoclinic channel $\Gamma \subset M$, and σ is the scattering map associated to Γ.*

Let $m_1, \dots, m_l \in \mathbb{N}$ be a fixed sequence of integers. Let $\{x_i\}_{i=0,\dots,l}$ be a finite pseudo-orbit in Λ, that is a sequence of points in Λ of the form

$$x_{i+1} = f^{m_i} \circ \sigma^{\Gamma}(x_i), \qquad i = 0, \dots, l-1,\ l \geq 1. \tag{9}$$

Then for every $\delta > 0$ there exists an orbit $\{z_i\}_{i=0,\dots,l}$ of f in M, with $z_{i+1} = f^{k_i}(z_i)$ for some $k_i > 0$, such that $d(z_i, x_i) < \delta$ for all $i = 0, \dots, l$.

Remark 6. *The result can be immediately extended to the case where we have a finite number of scattering maps $\sigma_1, \dots, \sigma_L$ to shadow*

$$x_{i+1} = f^{m_i} \circ \sigma_{\alpha_i}(x_i), \qquad i = 0, \dots, l-1,\ l \geq 1,$$

for two prescribed sequences $m_1, \dots, m_l \in \mathbb{N}$ and $\alpha_1, \dots, \alpha_l \in \{1, \dots, L\}$; see [4, Theorem 3.7].

Remark 7. *Theorem 5 has been simplified taking advantage of our particular setting. See comments in [6, Remark 6].*

2.4. Diffusion mechanism

In this section we recall the results from [6]. These are based on [4], but were adapted in [6] to allow for computer assisted validation of the required assumptions.

Consider the following family of Hamiltonian systems $H_\varepsilon : \mathbb{R}^4 \times \mathbb{T} \to \mathbb{R}$, that depends smoothly on the parameter $\varepsilon \in \mathbb{R}$, which generates the following ODE in the extended phase space

$$\begin{aligned} x' &= J \nabla_x H_\varepsilon(x, t), \\ t' &= 1, \end{aligned} \tag{10}$$

where

$$J = \begin{pmatrix} 0 & Id \\ -Id & 0 \end{pmatrix}, \qquad \text{for} \qquad Id = \begin{pmatrix} 1 & 0 \\ 0 & 1 \end{pmatrix}.$$

Let Φ_t^ε be the flow of (10). We refer to $H_{\varepsilon=0}$ as the unperturbed system. We make the following important assumption

$$H_{\varepsilon=0}(x, t) = H(x),$$

where $H : \mathbb{R}^4 \to \mathbb{R}$; in other words, we assume that the unperturbed system is autonomous and hence H is a constant of motion.

Consider a Poincaré section Σ in $\mathbb{R}^4$ for the system $x' = J \nabla H(x)$, and consider a section $\tilde{\Sigma} = \Sigma \times \mathbb{T}$ for the perturbed system (10) in the extended phase space. Let us consider a Pioncaré map

$$f_\varepsilon : \tilde{\Sigma} \to \tilde{\Sigma}. \tag{11}$$

We assume that for $\varepsilon = 0$ the map $f_{\varepsilon=0}$ has a normally hyperbolic invariant manifold $\Lambda_0 \subset \tilde{\Sigma}$.

The coordinates on $\tilde{\Sigma}$ can be identified with $\mathbb{R}^3 \times \mathbb{T}$. We will write $\theta \in \mathbb{T}$ for the extended phase space (time) coordinate. We assume that one of the remaining coordinates on $\tilde{\Sigma}$ is the energy, expressed by the Hamiltonian H. We will write I for this coordinate. Since for $\varepsilon = 0$ the energy is preserved we have

$$\pi_I f_0(z) = \pi_I z \qquad \text{for all } z \in \tilde{\Sigma}. \tag{12}$$

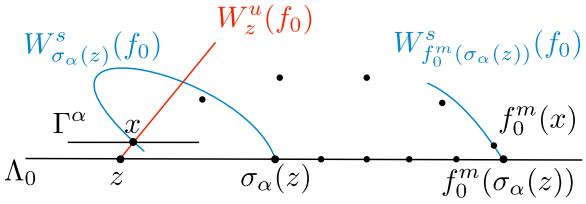

Figure 1: The setting for Theorem 9. [6]

We assume that Λ_0 is parameterised by θ, I. For the remaining two coordinates on $\tilde{\Sigma}$ we will write u and s and equip $\tilde{\Sigma}$ with the standard symplectic from $\omega = du \wedge ds + d\theta \wedge dI$. Due to the Hamiltonian nature of the system, the map f_ε is symplectic. We assume that

$$\Lambda_0 = \{(u, s, I, \theta) : u = s = 0\},$$

is a normally hyperbolic invariant manifold for f_0. The coordinates u and s stand for the 'unstable' and 'stable' coordinates of Λ_0, respectively. We assume also that for sufficiently small ε the manifold Λ_0 is perturbed to Λ_ε, which contains a Cantor set of one dimensional KAM invariant tori.

Let $g : \mathbb{R} \times \mathbb{R}^3 \times \mathbb{T} \to \mathbb{R}^3 \times \mathbb{T}$ be defined as

$$g(\varepsilon, x) := \frac{1}{\varepsilon}\left(f_\varepsilon(x) - f_0(x)\right).$$

Then

$$f_\varepsilon(x) = f_0(x) + \varepsilon g(\varepsilon, x).$$

The following theorem provides conditions under which for any sufficiently small $\varepsilon > 0$ there exists a point x_ε and a number of iterates n_ε for which

$$\pi_I\left(f_\varepsilon^{n_\varepsilon}(x_\varepsilon) - x_\varepsilon\right) > 1. \tag{13}$$

We first give a definition and follow with the statement of the theorem.

Definition 8. *Consider the topology on $\Lambda_0 \cap \{I \in [0,1]\}$ induced by Λ_0. We say that an open set $S \subset \Lambda_0 \cap \{I \in [0,1]\}$ is a strip in Λ_0 iff*

$$S \cap \{z \in \Lambda_0 : \pi_I z = \iota\} \neq \emptyset \qquad \text{for any } \iota \in [0,1].$$

Theorem 9. *[6] Assume that there is a neighborhood U of Λ_0 and a positive constant L_g such that for every $z \in \Lambda_0$, $x_u \in W^u_z(f_0, U)$, $x_s \in W^s_z(f_0, U)$,*

$$\begin{aligned} |\pi_I\left(g(0, x_u) - g(0, z)\right)| &\leq L_g \|x_u - z\|, \\ |\pi_I\left(g(0, x_s) - g(0, z)\right)| &\leq L_g \|x_s - z\|. \end{aligned} \tag{14}$$

Assume also that there exist positive constants C, λ, where $\lambda \in (0,1)$, such that for every $z \in \Lambda_0$ and every $x_u \in W^u_z(f_0, U)$, $x_s \in W^s_z(f_0, U)$ we have

$$\begin{aligned} \left\|f_0^n(z) - f_0^n(x_u)\right\| &< C\lambda^{|n|} \qquad \text{for all } n \leq 0, \\ \left\|f_0^n(z) - f_0^n(x_s)\right\| &< C\lambda^n \qquad \text{for all } n \geq 0. \end{aligned} \tag{15}$$

Assume also that for $\varepsilon = 0$ we have the sequence of scattering maps $\sigma_\alpha : \mathrm{dom}(\sigma_\alpha) \to \Lambda_0$ for $\alpha = 1, \ldots, L$. Let $S^+ \subset \Lambda_0$ be a strip. Assume that for every $z \in \overline{S^+}$

1. *there exists an $\alpha \in \{1, \ldots, L\}$ for which $z \in \mathrm{dom}(\sigma_\alpha)$, and there exists a constant $m \in \mathbb{N}$ such that*
$$f_0^m \circ \sigma_\alpha(z) \in S^+, \tag{16}$$
2. *there exists a point $x \in W_z^u(f_0, U) \cap W^s_{\sigma_\alpha(z)}(f_0)$ such that $f_0^m(x) \in W^s_{f_0^m(\sigma_\alpha(z))}(f_0, U)$ and*
$$\sum_{j=0}^{m-1} \pi_I g\left(0, f_0^j(x)\right) - \frac{1+\lambda}{1-\lambda} L_g C > 0. \tag{17}$$

(The choice of m and α can depend on z.)

Then for sufficiently small $\varepsilon > 0$ there exists an x_ε and $n_\varepsilon > 0$ such that
$$\pi_I\left(f_\varepsilon^{n_\varepsilon}(x_\varepsilon) - x_\varepsilon\right) > 1.$$

The following theorem can be used to establish orbits of the perturbed system, whose I coordinate decreases.

Theorem 10. *[6]Assume that conditions (14) and (15) are satisfied, and that for $\varepsilon = 0$ we have the sequence of scattering maps $\sigma_\alpha : \mathrm{dom}(\sigma_\alpha) \to \Lambda_0$ for $\alpha = 1, \ldots, L$. Let $S^- \subset \Lambda_0$ be a strip. Assume that for every $z \in \overline{S^-}$*

1. *there exists an $\alpha \in \{1, \ldots, L\}$ for which $z \in \mathrm{dom}(\sigma_\alpha)$, and there exists a constant $m \in \mathbb{N}$ such that*
$$f_0^m \circ \sigma_\alpha(z) \in S^-,$$
2. *there exists a point $x \in W_z^u(f_0, U) \cap W^s_{\sigma_\alpha(z)}(f_0)$ such that $f_0^m(x) \in W^s_{f_0^m(\sigma_\alpha(z))}(f_0, U)$ and*
$$\sum_{j=0}^{m-1} \pi_I g\left(0, f_0^j(x)\right) + \frac{1+\lambda}{1-\lambda} L_g C < 0.$$

(The choice of m and α can depend on z.)

Then for sufficiently small $\varepsilon > 0$ there exists an x_ε and $n_\varepsilon > 0$ such that
$$\pi_I\left(x_\varepsilon - f_\varepsilon^{n_\varepsilon}(x_\varepsilon)\right) > 1.$$

By combining the two strips S^+ and S^- we obtain shadowing of any prescribed finite sequence of actions.

Theorem 11. *[6] Assume that two strips S^+ and S^- satisfy assumptions of Theorems 9 and 10, respectively. If in addition*

1. *for every $z \in \overline{S^+}$ there exists an n (which can depend on z) such that $f_0^n(z) \in S^-$, and*
2. *for every $z \in \overline{S^-}$ there exists an n (which can depend on z) such that $f_0^n(z) \in S^+$,*

then there exists an $\mathcal{M}$ such that for any given finite sequence $\{I_k\}_{k=0}^N$ and any given $\delta > 0$, for sufficiently small ε there exists an orbit of f_ε which $\varepsilon\mathcal{M}$-shadows the actions I_k; i.e. there exists a point z_0^ε and a sequence of integers $n_1^\varepsilon \le n_2^\varepsilon \le \ldots \le n_N^\varepsilon$ such that
$$\left\| \pi_I f_\varepsilon^{n_k^\varepsilon}\left(z_0^\varepsilon\right) - I_k \right\| < \varepsilon\mathcal{M}.$$

2.5. The Planar Elliptic Restricted Three Body Problem

The Planar Elliptic Restricted Three Body Problem (PER3BP) describes the motion of a massless particle (e.g., an asteroid or a spaceship), under the gravitational pull of two large bodies, which we call primaries. The primaries rotate in a plane along Keplerian elliptical orbits with eccentricity ε, while the massless particle moves in the same plane and has no influence on the orbits of the primaries. We use normalized units, in which the masses of the primaries are μ and $1-\mu$. We consider a frame of 'pulsating' coordinates that rotates together with the primaries, making their position fixed on the horizontal axis [14]. The motion of the massless particle is described via the Hamiltonian $H_\varepsilon : \mathbb{R}^4 \times \mathbb{T} \to \mathbb{R}$

$$\begin{aligned} H_\varepsilon(X, Y, P_X, P_Y, \theta) &= \frac{(P_X + Y)^2 + (P_Y - X)^2}{2} - \frac{\Omega(X, Y)}{1 + \varepsilon\cos(\theta)}, \\ \Omega(X, Y) &= \frac{1}{2}\left(X^2 + Y^2\right) + \frac{(1-\mu)}{r_1} + \frac{\mu}{r_2}, \\ r_1^2 &= (X - \mu)^2 + Y^2, \\ r_2^2 &= (X - \mu + 1)^2 + Y^2. \end{aligned} \tag{18}$$

The corresponding Hamilton equations are:

$$\begin{aligned} \frac{dX}{d\theta} &= \frac{\partial H_\varepsilon}{\partial P_X}, & \frac{dP_X}{d\theta} &= -\frac{\partial H_\varepsilon}{\partial X}, \\ \frac{dY}{d\theta} &= \frac{\partial H_\varepsilon}{\partial P_Y}, & \frac{dP_Y}{d\theta} &= -\frac{\partial H_\varepsilon}{\partial Y}, \end{aligned} \tag{19}$$

where $X, Y \in \mathbb{R}$ are the position coordinates of the massless particle, and $P_X, P_Y \in \mathbb{R}$ are the associated linear momenta. The variable $\theta \in \mathbb{T}$ is the true anomaly of the Keplerian orbits of the primaries, where $\mathbb{T}$ denotes the 1-dimensional torus. The system is non-autonomous, thus we consider it in the extended phase space, of dimension 5, with θ as an independent variable. We use the notation Φ_t^ε to denote the flow of (19) in the extended phase space, which includes $\theta \in \mathbb{T}$, i.e.

$$\Phi_t^\varepsilon : \mathbb{R}^4 \times \mathbb{T}^1 \to \mathbb{R}^4 \times \mathbb{T}^1.$$

When $\varepsilon = 0$ the primaries rotate around the center of mass along circular orbits. The PER3BP becomes the Planar Circular Restricted Three Body Problem (PCR3BP). We shall use the notation Φ_t for the flow of the PCR3BP. Since the ODE of the PCR3BP is autonomous, this flow is not in the extended phase space, i.e. for a given $t \in \mathbb{R}$,

$$\Phi_t : \mathbb{R}^4 \to \mathbb{R}^4.$$

We naturally have the relation $\Phi_t(x) = \pi_x \Phi_t^0(x, \theta)$ (for $\varepsilon = 0$ the right hand side does not depend on the choice of θ).

In the PCR3BP the system has the following time reversing symmetry

$$\mathcal{R} \circ \Phi_t = \Phi_{-t} \circ \mathcal{R}, \tag{20}$$

where

$$\mathcal{R}(X, Y, P_X, P_Y) = (X, -Y, -P_X, P_Y).$$

We say that an orbit $x(t)$ is $\mathcal{R}$-symmetric if

$$x(-t) = \mathcal{R}(x(t)).$$

Note that for such orbits we need to have $\pi_Y x(0) = \pi_{P_X} x(0) = 0$.

The Jacobi integral $-2 \cdot H_0$ is a preserved coordinate for the unperturbed system with $\varepsilon = 0$. We shall refer to H_0 as the energy. For a point $x \in \mathbb{R}^4$ we shall write

$$I(x) := H_0(x).$$

3. Statement of the main result

The PCR3BP has five libration fixed points. Three of these are on $\{Y = 0\}$; we refer to them as collinear and denote as L_1, L_2, L_3. We use the convention, in which in the X, Y coordinates the Jupiter, with mass μ lies to the left of the origin at $(\mu - 1, 0)$, and the Sun, with mass $1 - \mu$ is to the right of the origin at $(\mu, 0)$. One of the collinear libration points, which we denote as L_1 lies between the Sun and Jupiter. Around this fixed point we have a family of Lyapunov periodic orbits. Each orbit has different energy. The Lyapunov orbits are $\mathcal{R}$-symmetric and we can choose points belonging to the orbits of the form $(X, 0, 0, P_X)$, with suitable choices of X and P_X. The P_X depends on the choice of X, so we shall write $P_X = P_X(X)$.

The Lyapunov orbits considered by us will be parameterised by X. From now on, we will write $\mathcal{X} \in \mathbb{R}$ to denote the value $X = \mathcal{X}$, which determines the choice of a point on the Lyapunov orbit $(\mathcal{X}, 0, 0, P_X(\mathcal{X}))$. This will allow us to make the distinction between $\mathcal{X}$, which are values parameterising the orbits and the coordinate X. We will be interested in the family of Lyapunov orbits with

$$\mathcal{X} \in \left[-0.95, -0.95 + 10^{-9}\right]. \tag{21}$$

The energy of such orbits, measured by the Jacobi integral, is approximately 3.03, which is the energy of the comet Oterma [15] that was observed in the Jupiter-Sun system. We choose to work with this particular energy, since it has a physical meaning of a known celestial body, but we could easily work with a different $\mathcal{X}$-interval than (21), since there is nothing special about the energy of Oterma. In fact, choosing a different energy level can make some technical aspects of the computer assisted proof easier. (We elaborate on this in Remark 46.) We fix an energy level of some physical object to show that the method can be applied in a concrete setting.

For each $\mathcal{X}$ from (21) the corresponding Lyapunov orbit has a different energy $I(\mathcal{X})$. We will show that for sufficiently small $\varepsilon > 0$, that is for the PER3BP, we can visit the arbitrary $I(\mathcal{X})$ for $\mathcal{X}$ from (21). We shall refer to these as diffusing orbits. Formally, the main result of this paper is as follows.

Theorem 12. *(Main theorem) Let $I(\mathcal{X})$ denote the energy of a Lyapunov orbit starting from a given Lyapunov orbit, i.e.*

$$I(\mathcal{X}) = H(\mathcal{X}, 0, 0, P_X(\mathcal{X})).$$

There exists a constant $\mathcal{M} > 0$ such that for an arbitrary (finite) sequence $\mathcal{X}_1, \ldots, \mathcal{X}_N$ from the interval (21) and for sufficiently small $\varepsilon > 0$, there exists a sequence $t_1^\varepsilon, \ldots, t_n^\varepsilon$ and a point x^ε such that

$$\left\| H\left(\Phi^\varepsilon_{t_i^\varepsilon}(x^\varepsilon)\right) - I(\mathcal{X}_i) \right\| < \varepsilon \mathcal{M} \qquad \text{for } i = 1, \ldots, N.$$

Remark 13. *The interval (21) is very narrow. The actual physical distance between the two points on the Lyapunov orbits on the section* $\{Y = 0\}$*, which correspond to endpoints of (21) is about* 1 *km. This means that the diffusion established by us is over a very narrow range, but it is not completely negligible.*

Remark 14. *The proof was performed with computer-assisted tools, and for the interval (21) it took 17 minutes, running on a single thread on a standard laptop. Our computer assisted proof could be performed on other* X*-intervals, which combined together would lead to diffusion over longer distances. Such proof could be performed by parallel computations on a cluster. We are more interested in the proof of concept rather than in obtaining long intervals by brute force, so we have not performed such validation.*

4. Proof of the main result

The proof is performed in the following steps:

1. establish the existence of the family of Lyapunov orbits, which will form the NHIM Λ_0,
2. establish bounds for the local stable/unstable manifolds of Λ_0,
3. prove that the stable and unstable manifolds of Λ_0 intersect transversally, and that we have a homoclinic channel along the intersection,
4. prove that Λ_0 is perturbed to Λ_ε, which contains a Cantor set of KAM tori.
5. apply Theorem 11 to obtain the existence of diffusing orbits.

Section 4.1 sets out a parallel shooting method, which is then used for the steps 1 and 3 in sections 4.2 and 4.4, respectively. Sections 4.3, 4.5 and 4.6 deal with steps 2, 4 and 5, respectively.

4.1. Parallel shooting for symmetric orbits

Here we consider the PCR3BP and work with the flow Φ_t in $\mathbb{R}^4$. Let us consider a C^1 function $p : \mathbb{R} \to \mathbb{R}^4$. For now we leave p unspecified. Later on, depending on the choice of p we will use the below method to establish either bounds on the points along a Lyapunov orbit, or for a homoclinic orbit to a Lyapunov orbit.

Let us define the following function

$$F : \mathbb{R} \times \mathbb{R} \times \underbrace{\mathbb{R}^4 \times \ldots \times \mathbb{R}^4}_{n} \to \underbrace{\mathbb{R}^4 \times \ldots \times \mathbb{R}^4}_{n} \times \mathbb{R} \times \mathbb{R},$$

as

$$\begin{aligned} &F(s, \tau, x_1, \ldots, x_n) := \\ &\left(\Phi_\tau(p(s)) - x_1, \Phi_\tau(x_1) - x_2, \ldots, \Phi_\tau(x_{n-1}) - x_n, \pi_Y \Phi_\tau(x_n), \pi_{P_X} \Phi_\tau(x_n)\right). \end{aligned} \tag{22}$$

We see that if we find a point $\mathbf{x}^* = (s, \tau, x_1, \ldots, x_n)$ such that

$$F(\mathbf{x}^*) = 0, \tag{23}$$

then by taking $x_0 = p(s)$ and $x_{n+1} = \Phi_\tau(x_n)$ we obtain

$$\Phi_\tau(x_i) = x_{i+1} \qquad \text{for } i = 0, \ldots, n.$$

Moreover, since

$$\pi_Y x_{n+1} = \pi_Y \Phi_\tau(x_n) = 0, \qquad \pi_{P_X} x_{n+1} = \pi_{P_X} \Phi_\tau(x_n) = 0,$$

we see that x_{n+1} is $\mathcal{R}$-symmetric, i.e. $x_{n+1} = \mathcal{R}(x_{n+1})$. If we now define $x_{n+k} = \mathcal{R}(x_{n+2-k})$, for $k = 2, \ldots, n+2$ then by (20) we will obtain an $\mathcal{R}$-symmetric orbit $x(t)$, which starts from $x(0) = x_0$, and for which

$$\Phi_\tau(x_i) = x_{i+1} \qquad \text{for } i = 0, \ldots, 2n+1.$$

Solving of (23) can be done by means of the Krawczyk method. The first step is to obtain an approximate solution of (23) by iterating (using non-rigorous numerics)

$$\mathbf{x}_{i+1} = \mathbf{x}_i - (DF(\mathbf{x}_i))^{-1} F(\mathbf{x}_i). \tag{24}$$

After a few iterates of (24) we obtain a point $\mathbf{x}$ around which we can construct a cube $\mathbf{X}$ and validate that we have the solution of (23) inside of $\mathbf{X}$ by using Theorem 1. (We take C as the non-rigorously computed inverse of the derivative $C = (DF(\mathbf{x}))^{-1}$.)

4.2. Bounds for Lyapunov orbits

When we fix some $\mathcal{X} \in \mathbb{R}$ and choose the function $p : \mathbb{R} \to \mathbb{R}^4$ as

$$p(s) = (\mathcal{X}, 0, 0, s), \tag{25}$$

then the methodology form section 4.1 can be used to obtain a sequence of points $x_0, \ldots, x_{2n+2}$ along an $\mathcal{R}$-symmetric periodic orbit. This is because by the definition of F

$$\Phi_{(n+1)\tau}(x_0) = x_{n+1},$$

and since x_0 and x_{n+1} are self $\mathcal{R}$-symmetric, by (20)

$$\Phi_{(n+1)\tau}(x_{n+1}) = \Phi_{(n+1)\tau} \circ \mathcal{R}(x_{n+1}) = \mathcal{R} \circ \Phi_{-(n+1)\tau}(x_{n+1}) = \mathcal{R}(x_0) = x_0.$$

We thus see that x_0 is a point on an $\mathcal{R}$-symmetric periodic orbit with period $T = 2(n+1)\tau$.

An advantage of the method is that we can obtain a bound for a whole family of Lyapunov orbits. This can be done by considering an interval instead of a single $\mathcal{X}$, for our validation. The computer assisted computation allows us to obtain a bound on $F(x)$ and $DF(x)$ for (22). This way we obtain a bound for points which lie on Lyapunov orbits for an interval of values $\mathcal{X}$. In our case we take the interval (21) and use this method to validate the following result:

Lemma 15. *Let $r := 3.633 \cdot 10^{-9}$. For every $\mathcal{X}$ from the interval (21) there exists an*

$$s(\mathcal{X}) \in -0.84134724633 + [-r, r]$$

such that

$$x_0(\mathcal{X}) = (\mathcal{X}, 0, 0, s(\mathcal{X})) \tag{26}$$

is a point, which lies on a Lyapunov orbit, which we denote as $L_{\mathcal{X}}$. Moreover, we have a sequence of points along $L_{\mathcal{X}}$, which passes within the r distance (in maximum norm) of the points from Table 1. Moreover, we have the following bound $T(\mathcal{X})$ for the period of $L_{\mathcal{X}}$

$$T(\mathcal{X}) \in [3.0417517493, 3.0417517846] \tag{27}$$

n	X	Y	P_X	P_Y
0	-0.9499999995	0	0	-0.84134724633
1	-0.95011002908	0.010872319337	-0.012750492306	-0.84566628682
2	-0.95027977734	0.020942127841	-0.021798848297	-0.85701977629
3	-0.95016249921	0.02964511208	-0.02595601236	-0.87222441368
4	-0.94945269037	0.036681290981	-0.026117965229	-0.88881047965
5	-0.94799596417	0.041912835694	-0.023738329652	-0.90554260324
6	-0.94578584443	0.045275924414	-0.020027448005	-0.92194698888
7	-0.94292354313	0.046741951127	-0.015815875271	-0.93784624844
8	-0.93958019632	0.046310536541	-0.011642040196	-0.9531124603
9	-0.93596962345	0.044016227704	-0.0078569213076	-0.96756323289
10	-0.93232909834	0.039939546482	-0.0046935571959	-0.98092506113
11	-0.92890403848	0.034218254755	-0.0022984843476	-0.99282861416
12	-0.92593321085	0.027056429274	-0.00073280826007	-1.0028268728
13	-0.92363228182	0.018728871729	4.5125264188e-05	-1.0104387689
14	-0.92217533629	0.0095779013399	0.00019712976878	-1.0152203731
15	-0.92167641746	0	0	-1.0168530766

Table 1: Midpoints of our enclosure of points along the family of Lyapunov orbits, computed using (23) with $n = 14$.

Remark 16. *In Table 1 we write out half of the points along the family of periodic orbits, since the second half (the remaining fourteen points, to be precise) follows from the $\mathcal{R}$-symmetry.*

Remark 17. *Our estimate on the distance from the points from Table 1 obtained by our computer program varies from point to point and is frequently more accurate than stated in Lemma 15, where we simply write out the single r, which is the upper bound that can be applied to all the points.*

4.3. Bounds on the unstable manifolds of Lyapunov orbits

In the previous section we have shown how to compute the bound on the family of Lyapunov orbits $L_{\mathcal{X}}$ containing points $x_0(\mathcal{X})$ given by (26), with $\mathcal{X}$ from the interval (21). Here we fix a single periodic orbit for some $\mathcal{X}$ from (21) and discuss how one can obtain a computer validated enclosure of its local unstable manifold. Before we give the method, we introduce some notation.

We consider a Poincaré section $\Sigma = \{Y = 0\}$ and define $\rho : \mathbb{R}^4 \to \mathbb{R}$ and $\mathcal{P} : \mathbb{R}^4 \to \mathbb{R}^4$ as

$$\rho(x) = \inf\{t > 0 : \Phi_t(x) \in \Sigma\},$$
$$\mathcal{P}(x) = \Phi_{\rho(x)}(x).$$

In other words, ρ is the time along the flow to the section, and $\mathcal{P}$ is the map which goes to the section along the flow.

Remark 18. *The ρ and $\mathcal{P}$ do not need to be globally defined. Whenever we will use these functions in our computer assisted proofs, the CAPD library verifies that the considered sets lie within the domains of these maps, and that they are properly defined throughout the performed validations. (If a set would not belong to the domain, the program would return an error and terminate.)*

Let us fix $\mathcal{X}$ from (21) and a Lyapunov orbit $L_{\mathcal{X}}$ containing $x_0 = x_0(\mathcal{X})$ given by (26). Denote the period of this orbit as $T = T(\mathcal{X})$. For convenience, let us write $N = 2n + 2$, so that for our points $x_0, \ldots, x_N$ on the Lyapunov orbit, whose bounds we established in Lemma 15 we have

$$\Phi_{T/N}(x_i) = x_{i+1} \qquad \text{for } i = 0, \ldots, N-1, \tag{28}$$
$$x_N = x_0.$$

Note that from (26) we see that $x_0 \in \Sigma$.

Let us consider now a sequence of invertible matrices $A_i \in \mathbb{R}^{4\times 4}$ for $i = 0, \ldots, N$, with $A_0 = A_N$ and define the following maps

$$f_i : \mathbb{R}^4 \to \mathbb{R}^4, \qquad \text{for } i = 1, \ldots, N,$$

as

$$\begin{aligned} f_i(v) &:= A_i^{-1}\left(\Phi_{T/N}\left(A_{i-1}v + x_{i-1}\right) - x_i\right), \qquad \text{for } i = 1, \ldots, N-1, \\ f_N(v) &:= A_N^{-1}\left(\mathcal{P}\left(A_{N-1}v + x_{N-1}\right) - x_N\right) = A_0^{-1}\left(\mathcal{P}\left(A_{N-1}v + x_{N-1}\right) - x_0\right). \end{aligned} \tag{29}$$

In other words, for $i = 1, \ldots, N-1$ we consider time shift maps along the flow, expressed in local coordinates around x_i. The last map, f_N, maps to the section $\Sigma = \{Y = 0\} \subset \mathbb{R}^4$. This means that $f_N \circ \ldots \circ f_1|_\Sigma : \Sigma \to \Sigma$. From (28) it follows that

$$f_i(0) = 0 \qquad \text{for } i = 1, \ldots, N.$$

For $F : \mathbb{R}^4 \to \mathbb{R}^4$ defined as

$$F = f_N \circ \ldots \circ f_1 \tag{30}$$

we see that the origin is a fixed point. Our objective will be to establish bounds on the unstable manifold of the origin. To be more precise, we shall establish bounds on the intersection of the unstable manifold of the Lyapunov orbit with Σ, which is the unstable manifold of the origin for the map $F|_\Sigma$.

First we introduce some notion.

Definition 19. *Let $\|\cdot\|$ be some norm in $\mathbb{R}^3$. Let $Q : \mathbb{R}^4 \to \mathbb{R}$ be the function*

$$Q(v_1, \ldots, v_4) = |v_1| - \|(v_2, v_3, v_4)\|. \tag{31}$$

We define the cone centered at a point $v \in \mathbb{R}^4$ as

$$Q^+(v) := \left\{w \in \mathbb{R}^4 : Q(w - v) \geq 0\right\}.$$

We consider a sequence of cones defined by $Q_i : \mathbb{R}^4 \to \mathbb{R}$, for $i = 0, \ldots, N$ and assume that

$$Q_N = Q_0.$$

We take the norms $\|\cdot\|_i$ for Q_i from (31) as

$$\|(x_1, x_2, x_3)\|_i = \max\left\{|x_1|/a_{i,1}, \ldots, |x_3|/a_{i,3}\right\}$$

where $a_{i,k} \in (0, 1)$ are fixed coefficients for $i = 1, \ldots, N$ and $k = 1, 2, 3$. In other words, we use different norms in (31) to define different cones. Note that $|y| \geq \|(x_1, x_2, x_3)\|_i$ is equivalent to $a_{i,k}|y| \geq |x_k|$, for $k = 1, 2, 3$, so the cone $Q_i^+(v)$ can be expressed as

$$Q_i^+(v) = \left\{v + (t, tx_1, tx_2, tx_3) : x_k \in \left[-a_{i,k}, a_{i,k}\right] \text{ for } k = 1, 2, 3 \text{ and } t \in \mathbb{R}\right\}. \tag{32}$$

Remark 20. *The form (32) is convenient, since then cones defined by Q_i^+ can be represented in a computer assisted implementation by a set*

$$V_i = [1] \times \left[-a_{i,1}, a_{i,1}\right] \times \ldots \times \left[-a_{i,3}, a_{i,3}\right].$$

What we mean by this is that

$$Q_i^+(v) = \{v + tw : w \in V_i \text{ and } t \in \mathbb{R}\}. \tag{33}$$

Definition 21. *Let $B \subset \mathbb{R}^4$. We say that f_i satisfies cone conditions in B iff for every $v \in B$*

$$f_i\left(Q_i^+(v) \cap B\right) \subset Q_{i+1}^+\left(f_i(v)\right). \tag{34}$$

Below lemma is our main tool for establishing bounds on the unstable manifold of the origin for the map (30).

Lemma 22. *[16, Lemma 6.3] Let $B := [-1,1]^4 \subset \mathbb{R}^4$. Assume that $f_1, \ldots, f_N$ satisfy cone conditions in B. Let $m > 1$ and assume that for $F = f_N \circ \ldots \circ f_1$ the matrix $DF(0)$ has a single eigenvalue λ satisfying $|\mathrm{Re}\,\lambda| > m$ and the absolute values of the real parts of the remaining eigenvalues below m. If also for every $v \in Q_i^+(0) \cap B$,*

$$\|f_i(v)\| > m\|v\|, \tag{35}$$

then the unstable manifold of the origin for the map F is parameterised as a smooth curve $p^{\mathrm{u}} : [-1,1] \to B$ which satisfies

$$\begin{aligned} p^{\mathrm{u}}(0) &= 0, \\ \pi_1 p^{\mathrm{u}} &= Id, \\ p^{\mathrm{u}}([-1,1]) \subset Q_0^+\left(p^{\mathrm{u}}(u)\right), &\qquad \text{for every } u \in [-1,1], \end{aligned}$$

and

$$\frac{d}{du} p^{\mathrm{u}}(u) \in Q_0^+(0), \qquad \text{for every } u \in [-1,1].$$

Remark 23. *In [16, Lemma 6.3] is stated for the setting where F is a full turn along the periodic orbit. Here we have a sequence of local maps, which when composed constitute the full turn. The proof in such setting is analogous to [16], by using the graph transform method. The only needed modification with respect to [16] is that here the graphs need to be propagated successively by $f_1, f_2, \ldots, f_N$, after which they return to the same local coordinates. The graph transform for each successive f_i follows from an identical construction as the one from [16] (which there is done for the single F). By composing the graph transforms for the successive f_i we obtain a graph transform for F.*

Remark 24. *The benefit of considering several maps and shooting is that this requires shorter integration times, which improves accuracy in the interval arithmetic computations. This is the only reason why we shoot between 29 points along Lyapunov orbits, instead of considering a single turn.*

Remark 25. *In our computer assisted proof, we choose A_0 so that the derivative of $F = f_N \circ \ldots \circ f_1$ at the origin is close to diagonal. The eigenvalues of F are $\lambda, \frac{1}{\lambda}, 1, 0$. (The zero comes from the fact that f_N maps to the section Σ.) We can validate the bound on λ by using the Gersgorin theorem. We choose the remaining A_i so that the derivatives of f_i at the origin are close to diagonal.*

Remark 26. *The validation of cone conditions is done as follows. Take an interval set V_i for which we have (33). Then by the mean value theorem the fact that*

$$\left[Df_i(B)\right] V_i \subset Q_{i+1}(0) \tag{36}$$

implies (34). To check (36) it is enough to compute the interval set $w = [Df_i(B)]\, V_i$ *and validate that*

$$\left[\frac{w}{\pi_1 w}\right] \subset V_{i+1}.$$

This means that the cone condition is straightforward to validate from the interval enclosure of the derivative of the map.

In our computer assisted proof we use the following lemma to validate (35) for the maximum norm.

Lemma 27. *Consider* $Q(v_1, \ldots, v_4) = |v_1| - \|(v_2, v_3, v_4)\|$ *with*

$$\|(x_1, x_2, x_3)\| = \max\{|x_1|/a_1, |x_1|/a_2, |x_3|/a_3\},$$

where $a_1, a_2, a_3 \in (0,1)$*. Take* $f : B \to \mathbb{R}^4$ *such that* $f(0) = 0$ *and let*

$$[Df(B)] = \begin{pmatrix} A_{11} & A_{12} \\ A_{21} & A_{22} \end{pmatrix}, \tag{37}$$

where A_{11}*,* A_{12}*,* A_{21} *and* A_{22} *are* 1×1*,* 1×3*,* 3×1 *and* 3×3 *interval matrices, respectively. If* $A_{11} > c > 0$ *and* $m = c - \|A_{12}\|_{\max} \max(a_1, a_2, a_3)$*, then*

$$\|f(v)\|_{\max} \geq m \|v\|_{\max} \qquad \text{for every } v \in Q^+(0) \cap B.$$

Proof. The proof is given in Appendix A. ■

A mirror result can be formulated to obtain a bound in the other direction. This is relevant for the method for obtaining the bound (14) outlined in Appendix C. We place this lemma here since it follows from similar arguments to Lemma 22.

Lemma 28. *Consider* $Q(v_1, \ldots, v_4) = |v_1| - \|(v_2, v_3, v_4)\|$ *with*

$$\|(x_1, x_2, x_3)\| = \max\{|x_1|/a_1, |x_1|/a_2, |x_3|/a_3\},$$

where $a_1, a_2, a_3 \in (0,1)$*. Take* $f : B \to \mathbb{R}^4$ *and let*

$$[Df(B)] = \begin{pmatrix} A_{11} & A_{12} \\ A_{21} & A_{22} \end{pmatrix}, \tag{38}$$

where A_{11}*,* A_{12}*,* A_{21} *and* A_{22} *are* 1×1*,* 1×3*,* 3×1 *and* 3×3 *interval matrices, respectively. If*

$$a := \max(a_1, a_2, a_3), \tag{39}$$

$$\bar{m} := \max\left(|A_{11}| + a\|A_{12}\|_{\max}, \|A_{21}\|_{\max} + a\|A_{22}\|_{\max}\right), \tag{40}$$

then

$$\|f(v)\|_{\max} \leq \bar{m} \|v\|_{\max} \qquad \text{for every } v \in Q^+(0) \cap B.$$

Proof. The proof is given in Appendix B. ■

Remark 29. *In practice, the term* A_{11} *in (37)–(38), is associated with hyperbolic expansion, and dominates in (40). Also, in our application the number a from (39) is small, so we obtain* $m \approx \bar{m} \approx |A_{11}|$*; naturally* $m < \bar{m}$*.*

With the aid of Lemma 22 we have validated the following result.

Lemma 30. *Let* $r = 3 \cdot 10^{-8}$*,* $B = [-r, r]^4$*, and let*

$$A_0 = \begin{pmatrix} 0.280324 & -0.220733 & 0.280324 & 0 \\ 0 & 0 & 0 & 0.816632 \\ 1 & 0 & -1 & -1 \\ -0.343269 & 1 & -0.343269 & 0 \end{pmatrix}. \tag{41}$$

Consider $L = 5 \cdot 10^{-6}$ *and cones defined as*

$$Q_0^+(v) = \{v + (t, tx_2, tx_3, tx_4) : x_k \in [-L, L] \text{ for } k = 2, 3, 4 \text{ and } t \in \mathbb{R}\}.$$

Then the unstable manifold of the origin for the map F *is parameterised as a smooth curve* $p^{\mathrm{u}} : [-r, r] \to B$ *which satisfies*

$$\begin{aligned} p^{\mathrm{u}}(0) &= 0, \\ \pi_1 p^{\mathrm{u}} &= Id, \\ p^{\mathrm{u}}([-r, r]) \subset Q_0^+(p^{\mathrm{u}}(u)), &\qquad \text{for every } u \in [-r, r], \end{aligned}$$

and

$$\frac{d}{du} p^{\mathrm{u}}(u) \in Q_0^+(0), \qquad \text{for every } u \in [-r, r].$$

Corollary 31. *The curve* $w^{\mathrm{u}}(u) := x_0 + A_0 p^{\mathrm{u}}(u)$ *lies on the unstable manifold of the Lyapunov orbit containing* x_0*. The curve* $w^{\mathrm{u}}(u)$ *is contained in* $x_0 + A_0 Q_0^+(0)$ *and* $\frac{d}{du} w^{\mathrm{u}}(u) \in A_0 V_0$ *where*

$$V_0 = \{1\} \times [-L, L] \times [-L, L] \times [-L, L].$$

Since to define F *in (30) we take* $f_N = \mathcal{P}$ *(see (29)), and* $\mathcal{P}$ *maps to* Σ*, we know that* $w^{\mathrm{u}}(u) \subset \Sigma$*.*

Remark 32. *The matrices* A_i *used for the coordinate changes as well as the cones* Q_i *are chosen automatically by our computer program. We do not write them out here, since the important bounds for the proof are at the point* $x_0 = x_0(\mathcal{X})$*, and are given in Lemma 30.*

Remark 33. *To validate assumption (35) of Lemma 22 we have used Lemmas 27 and obtaining* $m = 1.2767546773$*, for the bound from (35).*

Remark 34. *We have also obtained the following bound by using Lemma 28 for maps (29)*

$$\|f_i(v_i)\|_{\max} \le \bar{m} \|v_i\|_{\max} \qquad \text{for } v_i \in Q_i^+(0) \cap B \text{ and } i = 1, \ldots, N,$$

where $\bar{m} = 1.2767636743$*.*

So far we have discussed how to obtain a bound on the fiber for a fixed point at the origin of our section-to-section map F defined in (30). Such fixed point resulted from intersecting the Lyapunov orbit with $\{Y = 0\}$. In the future discussion we will need to consider the problem in the extended phase space, since the PER3BP is not autonomous. In the extended phase space the fixed point at the origin for F becomes an invariant curve $\{0\} \times \mathbb{T}$. The unstable fiber for a given point $(0, \lambda)$, with $\lambda \in \mathbb{T}$, on this curve is contained in the extended phase space. Since the return

times to the section $\{Y = 0\}$ differ from point to point, such fiber does not need to be contained in $\{\theta = \lambda\}$. Below we discuss a method with which we establish bounds on the unstable fibers of points from $\{0\} \times \mathbb{T}$ in the extended phase space.

To make the above discussion more precise, we consider the flow of the PCR3BP in the extended phase space and denote it as $\tilde{\Phi}_t$. We consider the Poincaré section $\tilde{\Sigma} = \{Y = 0\} = \Sigma \times \mathbb{T}$, define $\tilde{\rho} : \mathbb{R}^4 \times \mathbb{T} \to \mathbb{R}$ and define $\tilde{\mathcal{P}} : \mathbb{R}^4 \times \mathbb{T} \to \mathbb{R}^4 \times \mathbb{T}$ as

$$\begin{aligned} \tilde{\rho}(x) &= \inf\left\{t > 0 : \tilde{\Phi}_t(x) \in \tilde{\Sigma}\right\}, \\ \tilde{\mathcal{P}}(x) &= \tilde{\Phi}_{\tilde{\rho}(x)}(x). \end{aligned}$$

Let also $\tilde{A}_0$ be a 5×5 matrix defined as

$$\tilde{A}_0 = \begin{pmatrix} A_0 & 0 \\ 0 & 1 \end{pmatrix}, \tag{42}$$

where A_0 is from (41). We define $\tilde{F} : \tilde{\Sigma} \to \tilde{\Sigma}$ as

$$\tilde{F}(x, \theta) = \tilde{A}_0^{-1}\left(\tilde{\mathcal{P}}^2\left((x_0, 0) + \tilde{A}_0(x, \theta)\right) - (x_0, 0)\right).$$

Then $\{0\} \times \mathbb{T}$ becomes a an invariant curve for the map $\tilde{F}$. We will now show how to obtain bounds for the unstable fibers of a point $(0, \lambda)$ on such curve, in the extended phase space.

Lemma 35. *Let r and L be the constants considered in Lemma 30. Let $M \in \mathbb{R}$, $M > 0$. Consider cones in the extended phase space defined as*

$$\tilde{Q}_0^+(v) = \{v + (t, tx_2, tx_3, tx_4, t\theta) : x_k \in [-L, L] \text{ for } k = 2, 3, 4,\ \theta \in [-M, M] \text{ and } t \in \mathbb{R}\}.$$

If for every $\lambda \in \mathbb{T}$ the unstable eigenvector of $D\tilde{F}(0, \lambda)$ is contained in $\tilde{Q}_0^+(0)$ and if $\tilde{F}$ satisfies $\tilde{Q}_0^+$ cone conditions on $[-r, r]^4 \times \mathbb{T}$, then for every $\lambda \in \mathbb{T}$ the unstable fiber $W^u_{(0,\lambda)}(\tilde{F})$ is parameterised by $\tilde{p}^{\mathrm{u}}_\lambda : [-r, r] \to \mathbb{R}^4 \times \mathbb{T}$ satisfying (below p^{u} is the function established in Lemma 30)

$$\pi_{\mathbb{R}^4} \tilde{p}^{\mathrm{u}}_\lambda(u) = p^{\mathrm{u}}(u) \qquad \text{and} \qquad \tilde{p}^{\mathrm{u}}_\lambda(u) \in \tilde{Q}_0^+(0, \lambda) \qquad \text{for } u \in [-r, r]. \tag{43}$$

In particular

$$\left|\pi_\theta \tilde{p}^{\mathrm{u}}_\lambda(u) - \lambda\right| \leq rM. \tag{44}$$

For the family of Lyapunov orbits with $\mathcal{X}$ from the interval (21) we can take $M = 3$.

Proof. For every λ the unstable fiber $W^u_{(0,\lambda)}(\tilde{F})$ is tangent at $(0, \lambda)$ to the eigenvector of $D\tilde{F}(0, \lambda)$. This implies that sufficiently close to $(0, \lambda)$ this fiber is in $\tilde{Q}_0^+(0, \lambda)$. Every point $x \in W^u_{(0,\lambda)}(\tilde{F})$ can be expressed as $x = \tilde{F}^m(z)$ for an arbitrary $m \in \mathbb{N}$, and for some appropriate point $z = z(m) \in W^u_{\tilde{F}^{-m}(0,\lambda)}(\tilde{F})$. By taking sufficiently large m the point z can be chosen as close to $\{0\} \times \mathbb{T}$ as we want, which means that we can choose m large enough so that $z \in \tilde{Q}_0^+\left(\tilde{F}^{-m}(0, \lambda)\right)$. Since $z \in \tilde{Q}_0^+\left(\tilde{F}^{-m}(0, \lambda)\right)$, by the fact that $\tilde{F}$ satisfies cone condition we obtain that $x = \tilde{F}^m(z) \in \tilde{Q}_0^+(0, \lambda)$. This means that for $W^u_{(0,\lambda)}(\tilde{F}) \cap ([-r, r]^4 \times \mathbb{T}) \subset \tilde{Q}_0^+(0, \lambda)$. Since the PCR3BP is autonomous, $\pi_{\mathbb{R}^4} W^u_{(0,\lambda)}(\tilde{F})$ does not depend on λ, and is parameterised by $p^{\mathrm{u}}(u)$ from Lemma 30. We have thus established (43).

n	X	Y	P_X	P_Y
0	-0.95000000242	-0	-1.0427994645e-08	-0.84134724275
1	-0.94997599415	0.032508255048	-0.026407880234	-0.87841641186
2	-0.94367569216	0.046559121408	-0.016859552423	-0.93400981538
3	-0.93185570859	0.039269494574	-0.0043284590814	-0.98260192685
4	-0.9227740512	0.014134265524	0.00018569728993	-1.0132585163
5	-0.92342538156	-0.017741502784	-8.9504023812e-05	-1.0111198858
6	-0.9332873018	-0.041191398464	0.0054636769818	-0.97749478375
7	-0.94483412083	-0.046015557539	0.018549243384	-0.92767343656
8	-0.95017205833	-0.029473079334	0.025907589742	-0.87187283933
9	-0.95002477482	0.0043928225728	-0.0053602054156	-0.84205223945
10	-0.94968890529	0.035271238551	-0.026402429149	-0.88508159957
11	-0.94246936536	0.046807227358	-0.015244331177	-0.94027843983
12	-0.93053821073	0.037102593271	-0.003488949681	-0.9875100719
13	-0.92242610924	0.010464221796	-0.00019611370513	-1.0149474376
14	-0.92456420774	-0.021092391132	-0.00083603746	-1.0083700678
15	-0.93548053074	-0.042380742641	0.0047663014948	-0.97130987256
16	-0.94730307615	-0.043772642856	0.016236744567	-0.91841934035
17	-0.95320906454	-0.022318932226	0.012564889629	-0.85729285711
18	-0.96070049024	0.017216683341	-0.061196504134	-0.84499124342
19	-0.98081741509	0.044653406262	-0.11087155568	-0.94184521723
20	-1.0057774379	0.042684693077	-0.12465612254	-1.0610257866
21	-1.0281206713	0	0	-1.2112777154

Table 2: Midpoints of our enclosure o homoclinic orbits for our family of Lyapunov orbits.

The condition (44) follows from the fact that $\tilde{p}^{\mathrm{u}}_{\lambda}(u) \in \tilde{Q}^{+}_{0}(0,\lambda)$ by computing

$$\left|\pi_{\mathbb{T}}\tilde{p}^{\mathrm{u}}_{\lambda}(u) - \lambda\right| \leq M\left|\pi_{x_1}\tilde{p}^{\mathrm{u}}_{\lambda}(u)\right| = M\left|\pi_{x_1}p^{\mathrm{u}}(u)\right| = M|u| \leq rM.$$

With computer assistance, we have validated that for every $\mathcal{X}$ from the interval (21), the unstable eigenvector of $D\tilde{F}(0,\lambda)$ is contained in

$$\{1\} \times [-3\cdot 10^{-6}, 3\cdot 10^{-6}]^3 \times [2.7763408157, 2.7918430312] \subset \tilde{Q}^{+}_{0}(0).$$

We have also validated the cone conditions using the method described in Remark 26. ■

Remark 36. *By choosing $\tilde{A}_0$ more carefully, instead of just adding* 1 *in the lower diagonal term in (42), we could reduce the constant M in Lemma 35. We have opted for (42) for the sake of simplicity, since the established M is good enough for the proof of the main result.*

4.4. Intersection of stable/unstable manifolds of Lyapunov orbits

The way we establish intersection of the stable and unstable manifolds of Lyapunov orbits is similar to the method from section 4.2. We use the parallel shooting from section 4.1 combined with the bounds on the unstable manifold established in section 4.3. We fix $\mathcal{X}$ from (21) and consider $p : \mathbb{R} \to \mathbb{R}^4$ for the shooting operator (22) to be

$$p(s) = x_0(\mathcal{X}) + A_0 p^{\mathrm{u}}(s), \tag{45}$$

where p^{u} is the function from which parameterises the intersection of the unstable manifold of $L_{\mathcal{X}}$ with $\{Y = 0\}$, whose bounds we have obtained in Lemma 30. (The choice of A_0 and the bounds on $p^{\mathrm{u}}(s)$, together with its derivative are written out in Lemma 30).

By the $\mathcal{R}$-symmetry of the PCR3BP we know that $\mathcal{R}(p(s))$ is a point on the stable manifold of $L_{\mathcal{X}}$. If for F defined by (22) we validate that for some $s \in (0,1)$ and $h \in \mathbb{R}$ we have

$$F(s, h, x_1, \ldots, x_n) = 0,$$

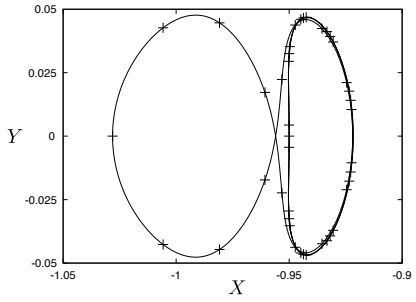

Figure 2: A homoclinic orbit to $L_{\mathcal{X}}$.

then taking $x_0 := p(s)$ and $x_{n+1} := \Phi_h(x_n)$ we obtain a sequence of points

$$x_0, \ldots, x_n, x_{n+1}, \mathcal{R}(x_n), \ldots, \mathcal{R}(x_0), \tag{46}$$

along an intersection of the stable and unstable manifolds of $L_{\mathcal{X}}$. With this method we have managed to obtain the following result.

Lemma 37. *For every $\mathcal{X}$ from (21) the stable and unstable manifolds of $L_{\mathcal{X}}$ intersect. Moreover, the intersection is along a $\mathcal{R}$-symmetric homoclinic orbit, which contains a sequence of points along it that lies $r = 1.96 \cdot 10^{-7}$ close to the orbit written out in Table 2; see also Figure 2.*

Remark 38. *In Table 2 we write out half of the points along the homoclinic, since the second half (the remaining twenty one points, to be precise) follows from the $\mathcal{R}$-symmetry.*

Remark 39. *Our estimate on the distance from the points from Table 2 obtained by our computer program varies from point to point and is frequently more accurate than stated in Lemma 37, where we simply write out the single r, which is the upper bound that can be applied to all the points.*

Remark 40. *From the method we also obtain a bound on the integration time h between the consecutive points along the homoclinic. We have obtained that*

$$h \in [0.34246881126, 0.34246888642]. \tag{47}$$

We now show that the established intersection is transversal.

Lemma 41. *For every $\mathcal{X}$ from the interval (21) the intersection of the stable and unstable manifolds of $L_{\mathcal{X}}$ is transversal when considered in the three dimensional constant energy level.*

Proof. We consider $\Sigma_{\{X<-1\}} = \{Y = 0, X < -1\} \subset \mathbb{R}^4$ and we will study the intersections of the stable/unstable manifolds of $L_{\mathcal{X}}$ on this section. (See Figure 2.)

Let us denote by $W^u_{L_{\mathcal{X}}}$ and $W^s_{L_{\mathcal{X}}}$ the unstable and stable manifolds of $L_{\mathcal{X}}$, respectively. These are two dimensional tubes, contained in the three dimensional constant energy level $\{H = h^*\}$ for $h^* = H(L_{\mathcal{X}})$. We have established that $W^u_{L_{\mathcal{X}}}$ and $W^s_{L_{\mathcal{X}}}$ intersect along a homoclinic orbit, which passes through the points (46). The point x_{n+1} belongs to $\Sigma_{\{X<-1\}}$. (From (22) we know that

$\pi_Y x_{n+1} = 0$ and from Table 2 we see that $\pi_X x_{n+1} < -1$, so $x_{n+1} \in \Sigma_{\{X<-1\}}$.) The vector field at x_{n+1} has a non zero Y-component. This means that the tangent spaces to the stable and unstable manifolds at x_{n+1} span the coordinate Y.

The manifolds $W^u_{L_\mathcal{X}}$ and $W^s_{L_\mathcal{X}}$ intersect with $\Sigma_{\{X<-1\}}$ at x_{n+1} along one dimensional curves. (Note that some of the points from the unstable/stable manifolds can collide with Jupiter. Those that reach $\Sigma_{\{X<-1\}}$ close to x_{n+1} intersect the section along one dimensional curves.) The section $\Sigma_{\{X<-1\}}$ is three dimensional, but $L_\mathcal{X}$, $W^u_{L_\mathcal{X}}$ and $W^s_{L_\mathcal{X}}$ are contained in $\{H = h^*\}$. The set $\Sigma_{\{X<-1\}} \cap \{H = h^*\}$ is two dimensional and can be parameterised[3] by coordinates (X, P_X). The $W^u_{L_\mathcal{X}} \cap \Sigma_{\{X<-1\}}$ and $W^s_{L_\mathcal{X}} \cap \Sigma_{\{X<-1\}}$ are therefore one dimensional curves contained in a two dimensional space, parameterised by (X, P_X), and if we show that

$$\pi_{X,P_X}\left(W^u_{L_\mathcal{X}} \cap \Sigma_{\{X<-1\}}\right) \quad \text{intersect transversally with} \quad \pi_{X,P_X}\left(W^s_{L_\mathcal{X}} \cap \Sigma_{\{X<-1\}}\right) \quad \text{at } x_{n+1}, \tag{48}$$

then we will obtain transversal intersections of $W^u_{L_\mathcal{X}}$ with $W^s_{L_\mathcal{X}}$ at x_{n+1} in $\{H = h^*\}$. (In more detail: the vector field at x_{n+1} is tangent to $W^u_{L_\mathcal{X}}$ and $W^s_{L_\mathcal{X}}$ at x_{n+1} and has a non zero Y-component; from (48) we will have that the tangent spaces to $W^u_{L_\mathcal{X}}$ and $W^s_{L_\mathcal{X}}$ at x_{n+1} span X, P_X. In all we span a three dimensional vector space, hence the intersection is transversal in $\{H = h^*\}$.)

Let $\tau : \mathbb{R}^4 \to \mathbb{R}, \mathcal{P} : \mathbb{R}^4 \to \Sigma_{\{X<-1\}}$ be defined as

$$\begin{aligned} \tau(x) &:= \inf\left\{t > 0 : \Phi_t(x) \in \Sigma_{\{X<-1\}}\right\}, \\ \mathcal{P}(x) &:= \Phi_{\tau(x)}(x). \end{aligned}$$

The curve $W^u_{L_\mathcal{X}} \cap \Sigma_{\{X<-1\}}$ can be obtained by computing $\mathcal{P} \circ p(s)$. (See (45) for the definition of $p(s)$.) By the $\mathcal{R}$-symmetry of the PCR3BP the $W^s_{L_\mathcal{X}} \cap \Sigma_{\{X<-1\}}$ is equal to $\mathcal{R} \circ \mathcal{P} \circ p(s)$. Let $s^* \in \mathbb{R}$ be such that $\mathcal{P} \circ p(s^*) = x_{n+1}$. If we establish that

$$\pi_X \frac{d}{ds} \mathcal{P} \circ p(s)|_{s=s^*} > 0 \qquad \text{and} \qquad \pi_{P_X} \frac{d}{ds} \mathcal{P} \circ p(s)|_{s=s^*} > 0, \tag{49}$$

then

$$\pi_X \frac{d}{ds} \mathcal{R} \circ \mathcal{P} \circ p(s)|_{s=s^*} = \pi_X \frac{d}{ds} \mathcal{P} \circ p(s)|_{s=s^*} > 0, \tag{50}$$

$$\pi_{P_X} \frac{d}{ds} \mathcal{R} \circ \mathcal{P} \circ p(s)|_{s=s^*} = -\pi_{P_X} \frac{d}{ds} \mathcal{P} \circ p(s)|_{s=s^*} < 0, \tag{51}$$

and from (49–51) we will obtain (48).

In section 4.3 we have established that (see Lemma 30 and Corollary 31)

$$\frac{d}{ds} p(s) \in \tilde{A}_0 V_0, \tag{52}$$

where V_0 is a set

$$V_0 = \{1\} \times [-L, L] \times [-L, L] \times [-L, L],$$

with $L = 5 \cdot 10^{-6}$. The set V_0 represents a cone, as described in Remark 20. We can propagate the bound (52) to the point x_{n+1} using cone propagation method described in Remark 26. We have thus validated that

$$\pi_{X,P_X} \frac{d}{ds} \mathcal{P} \circ p(s)|_{s=s^*} \in \{uV \,|\, u > 0 \text{ and } V = \{1\} \times [4.06081, 4.06404]\}.$$

This establish (49) and finishes our proof. ■

[3] On $\Sigma_{\{X<-1\}}$ the coordinate P_Y can be computed from X, P_X since $H(X, Y = 0, P_X, P_Y) = h^*$.

4.5. Persistence of the family of Lyapunov orbits

Recall that a Lyapunov orbit starting from $x_0(\mathcal{X})$ (see (26)), which has a period $T(\mathcal{X})$, is given as

$$L_{\mathcal{X}} = \{\Phi_t\left(x_0(\mathcal{X})\right) : t \in [0, T(\mathcal{X})]\}.$$

Let us denote the normally hyperbolic invariant manifold consisting of the family of Lyapunov orbits as

$$\Lambda_L = \{L_{\mathcal{X}} : \mathcal{X} \text{ are from the interval (21)}\} \subset \mathbb{R}^4.$$

We shall also use the following notation for the manifold in the extended phase space:

$$\tilde{\Lambda}_L = \Lambda_L \times \mathbb{T}. \tag{53}$$

To prove persistence of $\tilde{\Lambda}_L$ we shall use the following theorem:

Theorem 42. *[10] Assume that*

$$\frac{d}{d\mathcal{X}} T(\mathcal{X}) \neq 0 \tag{54}$$

and also

$$\frac{d}{d\mathcal{X}} H(x_0(\mathcal{X})) \neq 0. \tag{55}$$

Then for sufficiently small perturbation ε from the PCR3BP to the PER3BP, the manifold $\tilde{\Lambda}_L$ is perturbed into a $O(\varepsilon)$ close normally hyperbolic manifold $\tilde{\Lambda}_L^{\varepsilon}$, with boundary, which is invariant under the flow induced by (19). Moreover, there exists a Cantor set of invariant tori in $\tilde{\Lambda}_L^{\varepsilon}$.

We now discuss how we validate (54–55). Let us fix a single $\mathcal{X}$ from (26). From section 4.2 we know that there exists a $\tau = \tau(\mathcal{X})$, and an even[4] $N \in \mathbb{N}$, such that for $\tau = \tau(\mathcal{X})$ and for

$$\begin{aligned} x_0 &= x_0(\mathcal{X}) = (\mathcal{X}, 0, 0, s(\mathcal{X})), \\ x_{i+1} &= \Phi_\tau(x_i) \qquad \text{for } i = 0, \ldots, N-1 \end{aligned}$$

we have

$$x_N = x_0,$$

and the period of the Lyapunov orbit starting from x_0 is $T(\mathcal{X}) = N\tau(\mathcal{X})$.

Above was established by fixing $\mathcal{X}$ and solving for τ and s the following equation

$$\pi_{Y,P_X} \Phi_{\tau N/2}(\mathcal{X}, 0, 0, s) = 0. \tag{56}$$

(See (22) and (25); equation (22) provides us with the solution of (56) using parallel shooting.)

We can now define a function $g : \mathbb{R}^3 \to \mathbb{R}^2$ as

$$g(\mathcal{X}, s, \tau) = \pi_{Y,P_X} \Phi_{N\tau/2}(\mathcal{X}, 0, 0, s)$$

and observe that

$$g(\mathcal{X}, s(\mathcal{X}), \tau(\mathcal{X})) = 0. \tag{57}$$

[4] In our case we take $N = 30$, see Table 1.

This means that we can compute the derivatives of $\frac{ds}{d\mathcal{X}}$ and $\frac{d\tau}{d\mathcal{X}}$ from the implicit function theorem; i.e. by differentiating (57) with respect to $\mathcal{X}$ we obtain

$$\frac{\partial g}{\partial \mathcal{X}} + \frac{\partial g}{\partial (s,\tau)} \begin{pmatrix} \frac{ds}{d\mathcal{X}} \\ \frac{d\tau}{d\mathcal{X}} \end{pmatrix} = 0,$$

and provided that $\frac{\partial g}{\partial(s,\tau)}$ is invertible we see that

$$\begin{pmatrix} \frac{ds}{d\mathcal{X}} \\ \frac{d\tau}{d\mathcal{X}} \end{pmatrix} = -\left(\frac{\partial g}{\partial (s,\tau)}\right)^{-1} \frac{\partial g}{\partial \mathcal{X}}. \tag{58}$$

The partials $\frac{\partial g}{\partial \mathcal{X}}$, $\frac{\partial g}{\partial s}$ and $\frac{\partial g}{\partial \tau}$ are 2×1 matrices, which can be computed as follows. Let $e_i \in \mathbb{R}^4$, for $i = 1,\dots,4$, be a vector with 1 on i-th coordinate and zeros on the remaining coordinates. Let $\mathcal{F} : \mathbb{R}^4 \to \mathbb{R}^4$ stand for the vector field of the PCR3BP. Then

$$\frac{\partial g}{\partial \mathcal{X}}(x_0) = \pi_{Y,P_X} D\Phi_{N\tau/2}(x_0)\, e_1 = \pi_{Y,P_X} D\Phi_\tau(x_{N/2-1}) \dots D\Phi_\tau(x_0)\, e_1, \tag{59}$$

$$\frac{\partial g}{\partial s}(x_0) = \pi_{Y,P_X} D\Phi_{N\tau/2}(x_0)\, e_4 = \pi_{Y,P_X} D\Phi_\tau(x_{N/2-1}) \dots D\Phi_\tau(x_0)\, e_4, \tag{60}$$

$$\frac{\partial g}{\partial \tau}(x_0) = \frac{d}{d\tau}\pi_{X,P_X}\Phi_{N\tau/2}(x_0) = \frac{N}{2}\pi_{Y,P_X}\mathcal{F}\left(\Phi_{N\tau/2}(x_0)\right) = \frac{N}{2}\pi_{Y,P_X}\mathcal{F}\left(x_{N/2}\right). \tag{61}$$

Note that from the above $\frac{\partial g}{\partial s}$ and $\frac{\partial g}{\partial \tau}$ we obtain $\frac{\partial g}{\partial(s,\tau)} = \begin{pmatrix} \frac{\partial g}{\partial s} & \frac{\partial g}{\partial \tau} \end{pmatrix}$, which we can use in (58) to compute $\frac{ds}{d\mathcal{X}}$ and $\frac{d\tau}{d\mathcal{X}}$.

Once $\frac{ds}{d\mathcal{X}}$ is established, we can easily compute

$$\frac{dH}{d\mathcal{X}}(x_0(\mathcal{X})) = \frac{\partial H}{\partial X}(x_0(\mathcal{X})) + \frac{\partial H}{\partial P_Y}(x_0(\mathcal{X}))\frac{ds}{d\mathcal{X}}(\mathcal{X}). \tag{62}$$

We have used (58–62) to validate, with computer assistance, that we have the following:

Lemma 43. *For every $\mathcal{X}$ from (21) we have*

$$\begin{aligned}
\frac{d}{d\mathcal{X}} x_0(\mathcal{X}) &\in \{1\}\times\{0\}\times\{0\}\times[-4.530367, -4.530349], \\
\frac{d}{d\mathcal{X}}\tau(\mathcal{X}) &\in [-0.5523403, -0.5522624], \\
\frac{d}{d\mathcal{X}} T(\mathcal{X}) &\in [-16.57021, -16.56787], \\
\frac{d}{d\mathcal{X}} H(x_0(\mathcal{X})) &\in [-0.359187, -0.359185].
\end{aligned}$$

Corollary 44. *By Theorem 42 and Lemma 43 we obtain the persistence of the normally hyperbolic manifold $\tilde{\Lambda}_L$ (see (53)), which consists of our family of Lyapunov orbits in the extended phase space.*

4.6. Proof of the main theorem

Recall that Φ_t^ε is the flow of the PER3BP in the extended phase space. Let $\rho^\varepsilon : \mathbb{R}^4 \times \mathbb{T} \to \mathbb{R}$ be the time to the section $\{Y = 0\}$

$$\rho^\varepsilon(x) = \inf\{t > 0 : \Phi_t^\varepsilon(x) \in \{Y = 0\}\},$$

and let $\mathcal{P}_\varepsilon : \mathbb{R}^4 \times \mathbb{T} \to \{Y = 0\}$ be defined as

$$\mathcal{P}_\varepsilon(x) = \Phi^\varepsilon_{\rho(x)}(x). \tag{63}$$

The section $\{Y = 0\}$ in the extended phase space is isomorphic with $\mathbb{R}^3 \times \mathbb{T}$, which fits the setting from section 2.4.

We consider a single point $x^* := x_0(-0.95)$ ($x_0(\mathcal{X})$ is defined in (26); see also (21) regarding the choice of -0.95) and consider the matrix $\tilde{A}_0$ from (42). We define

$$\tilde{\Sigma} = \left\{\tilde{A}_0^{-1}(x - x^*, \theta) : x \in \{Y = 0\}, \theta \in \mathbb{T}\right\}.$$

In other words, $\tilde{\Sigma}$ is the section $\{Y = 0\}$ considered in the extended phase space, in the local coordinates given by the affine change given by x^* and $\tilde{A}_0$. We decide to work in these local coordinates since then we can directly use the estimates on the local unstable manifolds, which were established in section 4.3. This is the reason why we choose $\tilde{\Sigma}$ as above.

To apply Theorem 11 we will choose our family of maps (11)

$$f_\varepsilon : \tilde{\Sigma} \to \tilde{\Sigma}$$

to be defined as

$$f_\varepsilon(x, \theta) = \tilde{A}_0^{-1}\left(\mathcal{P}_\varepsilon \circ \mathcal{P}_\varepsilon\left((x^*, 0) + \tilde{A}_0(x, \theta)\right) - (x^*, 0)\right). \tag{64}$$

In other words, we consider the return map to the section $\{Y = 0\}$ expressed in our local coordinates.

Remark 45. *The reason for taking a composition of two $\mathcal{P}_\varepsilon$ in (64) is that for $\varepsilon = 0$ a Lyapunov orbit intersects $\{Y = 0\}$ in two points; or to be more precise, for $\varepsilon = 0$ a Lyapunov orbit becomes an invariant torus in the extended phase space, which intersects $\{Y = 0\}$ along two disjoint curves. (See Figure 3.) When working with $\mathcal{P}_\varepsilon \circ \mathcal{P}_\varepsilon$, each of these curves becomes an invariant circle for $f_{\varepsilon=0}$.*

Prior to the perturbation, for $\varepsilon = 0$, we define our normally hyperbolic invariant manifold $\Lambda_0 \subset \tilde{\Sigma}$ as (see (53) for the definition of $\tilde{\Lambda}_L$)

$$\Lambda_0 := \tilde{\Lambda}_L \cap \tilde{\Sigma}.$$

The manifold Λ_0 is foliated by invariant circles for the map f_0. Note that for $\varepsilon = 0$ the energy is preserved, so for

$$I(x) := H_0\left((x^*, 0) + \tilde{A}_0 x\right) \tag{65}$$

we see that

$$I(f_0(x)) = I(x). \tag{66}$$

We treat I as our conserved variable when $\varepsilon = 0$ and write

$$\pi_I x = I(x).$$

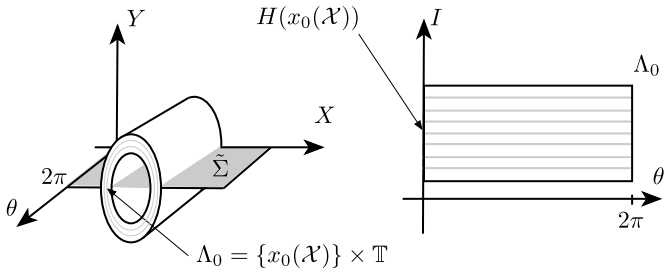

Figure 3: The manifold Λ_0 projected onto coordinates (X, Y, θ) on the left, and in coordinates (I, θ) on the right.

Thus, condition (66) plays the role of (12).

We can write f_ε as

$$f_\varepsilon(x) = f_0(x) + \varepsilon g(\varepsilon, x)$$

where

$$g(\varepsilon, x) = \frac{1}{\varepsilon}\left(f_\varepsilon(x) - f_0(x)\right). \tag{67}$$

To compute the change of the energy after an iterate of $f_\varepsilon(x)$ we compute

$$\pi_I f_\varepsilon(x) = \pi_I f_0(x) + \varepsilon \pi_I g(\varepsilon, x) = \pi_I x + \varepsilon \pi_I g(\varepsilon, x),$$

where $\pi_I g(\varepsilon, x)$ is

$$\pi_I g(\varepsilon, x) = \frac{1}{\varepsilon}\left[I(f_\varepsilon(x)) - I(f_0(x))\right] = \frac{1}{\varepsilon}\left[I(f_\varepsilon(x)) - I(x)\right].$$

It follows from the above that

$$\pi_I g(0, x) = \frac{d}{d\varepsilon} I(f_\varepsilon(x))|_{\varepsilon=0} = DI(f_0(x)) \frac{\partial f_0}{\partial \varepsilon}(x) = \nabla I(f_0(x)) \cdot \frac{\partial f_0}{\partial \varepsilon}(x). \tag{68}$$

(In the above equation $\cdot$ is the scalar product.)

We are now ready for the proof of our main result.

Proof of Theorem 12. We start by describing our system for $\varepsilon = 0$. While discussing the system for $\varepsilon = 0$ we will recall some results for the PCR3BP established in the previous sections. We need to keep in mind that these were considered in coordinates $(X, Y, P_X, P_Y) \in \mathbb{R}^4$; without the extended time coordinate θ.

The manifold Λ_0 is invariant under f_0 and in coordinates X, Y, P_X, P_Y, θ can be written as

$$\Lambda_0 = \{(x_0(\mathcal{X}), \theta) : \mathcal{X} \text{ is from (21)}, \theta \in \mathbb{T}\} \subset \mathbb{R}^4 \times \mathbb{T}.$$

For $\varepsilon = 0$ the inner dynamics produced by f_0 on the manifold is given as

$$(x_0(\mathcal{X}), \theta) \mapsto (x_0(\mathcal{X}), \theta + T(\mathcal{X})), \tag{69}$$

where $T(\mathcal{X})$ is the period of the Lyapunov orbit $L_\mathcal{X}$. Thus Λ_0 is an invariant cylinder, foliated by invariant curves.

Recall that for a given single Lyapunov orbit $L_{\mathcal{X}}$, we have established in Lemma 30 the bounds on a curve $p^{\mathrm{u}}(u)$, with $u \in (-r, r)$, which lies along the intersection of the two dimensional local unstable manifold of $L_{\mathcal{X}}$ (for the PCR3BP in $\mathbb{R}^4$) with the section $\{Y = 0\}$. Let us emphasize the dependence of $p^{\mathrm{u}}(u)$ on $\mathcal{X}$ by writing $p^{\mathrm{u}}_{\mathcal{X}}(u)$. The unstable manifold of Λ_0 for f_0, considered in $\{Y = 0\}$ (in the extended phase space) is three dimensional, and in the coordinates X, P_X, P_Y, θ, can locally be written as

$$W^u_{\Lambda_0} = \left\{ \left(p^{\mathrm{u}}_{\mathcal{X}}(u), \theta \right) : \ \mathcal{X} \text{ is from (21)}, u \in (-r, r), \theta \in \mathbb{T} \right\}.$$

By considering the $\mathcal{R}$-symmetry of the PCR3BP, in the extended phase space, and restricted to $\{Y = 0\}$, i.e.

$$\tilde{\mathcal{R}}(X, P_X, P_Y, \theta) := (X, -P_X, P_Y, \theta),$$

we obtain the local stable manifold

$$W^s_{\Lambda_0} = \tilde{\mathcal{R}}\left(W^u_{\Lambda_0} \right).$$

We will now show that for $\varepsilon = 0$ we have a well defined (and global) scattering map

$$\sigma : \Lambda_0 \to \Lambda_0. \tag{70}$$

For this we first need to establish a homoclinic channel. By Lemmas 37, 41 we know that the two dimensional stable and unstable manifolds of $L_{\mathcal{X}}$ in the PCR3BP in $\mathbb{R}^4$ intersect transversally (when considered on a three dimensional fixed energy set $\{H_0 = I\}$, where $I = H_0(L_{\mathcal{X}})$) along an $\mathcal{R}$-symmetric homoclinic orbit, which contains a point which we shall denote here as $\gamma(I) \in \{Y = 0\}$. The two dimensional stable and unstable manifolds of a given Lyapunov orbit $L_{\mathcal{X}}$, when intersected with $\{Y = 0\}$, become one dimensional curves in $\{Y = 0\}$ which intersect at $\gamma(I)$. Let us denote these curves as $w^{\mathrm{u}}_I(u)$ and $w^{\mathrm{s}}_I(s)$, and work under a convention that $w^{\mathrm{u}}_I(0) = w^{\mathrm{s}}_I(0) = \gamma(I)$. (This can always be ensured by re-parameterising the curves.) We have added the subscript I to emphasize the dependence of the curves on the choice of the energy level: on different energy levels we have a different Lyapunov orbits, that lead to different curves. We have shown during the proof of Lemma 41 that the tangent vectors to these curves span the X, P_X plane, i.e.

$$\operatorname{span}\left(\pi_{X,P_X} \frac{d}{du} w^{\mathrm{u}}_I(u)|_{u=0}, \pi_{X,P_X} \frac{d}{ds} w^s_I(s)|_{s=0} \right) = \mathbb{R}^2. \tag{71}$$

We shall take

$$\Gamma := \{ (\gamma(I), \theta) : \ I = H_0(L_{\mathcal{X}}), \mathcal{X} \text{ is from (21) and } \theta \in \mathbb{T} \} \subset \tilde{\Sigma} \tag{72}$$

and prove that it is a well defined homoclinic channel by showing (5–8).

It will be convenient for us to check the transversality conditions (5–8) in coordinates X, P_X, I, θ. In these coordinates we can parameterise Λ_0 by I, θ (see Figure 3)

$$\Lambda_0 = \{ (\pi_{X,P_X} x_0(\mathcal{X}), I, \theta) : I \in \mathbb{R}, \ \theta \in \mathbb{T}, \ H_0(L_{\mathcal{X}}) = I \}.$$

Close the intersection of the stable and unstable manifold at $(\gamma(I), \theta)$, we can parameterise the manifold $W^u_{\Lambda_0}$ by I, θ, u as follows

$$W^u_{\Lambda_0} = \{ (\pi_{X,P_X} w^{\mathrm{u}}_I(u), I, \theta) : I \in \mathbb{R}, \ \theta \in \mathbb{T}, \ u \in \mathbb{R} \}.$$

We can similarly parameterise the manifold $W^u_{\Lambda_0}$ by I, θ, s

$$W^s_{\Lambda_0} = \{(\pi_{X,P_X} w^{\mathrm{s}}_I(s), I, \theta) : I \in \mathbb{R},\ \theta \in \mathbb{T},\ s \in \mathbb{R}\},$$

and parameterise Γ by I, θ as in (72). We see that at a point $(\gamma(I), \theta) \in \Gamma$

$$T_{(\gamma(I),\theta)} W^u_{\Lambda_0} = \operatorname{span}\left\{\left(\pi_{X,P_X}\frac{d}{du} w^{\mathrm{u}}_I(u)|_{u=0}, 0, 0\right), \left(\pi_{X,P_X}\frac{d}{dI} w^{\mathrm{u}}_I(0), 1, 0\right), (0,0,0,1)\right\}, \tag{73}$$

$$T_{(\gamma(I),\theta)} W^s_{\Lambda_0} = \operatorname{span}\left\{\left(\pi_{X,P_X}\frac{d}{ds} w^{\mathrm{s}}_I(s)|_{s=0}, 0, 0\right), \left(\pi_{X,P_X}\frac{d}{dI} w^{\mathrm{s}}_I(0), 1, 0\right), (0,0,0,1)\right\}, \tag{74}$$

$$T_{(\gamma(I),\theta)} \Gamma = \operatorname{span}\left\{\left(\pi_{X,P_X}\frac{d}{dI}\gamma(I), 1, 0\right), (0,0,0,1)\right\}. \tag{75}$$

We know that $\gamma(I)$ results from the intersection of $w^{\mathrm{u}}_I(u)$ and $w^{\mathrm{s}}_I(s)$ at $u = s = 0$

$$\gamma(I) = w^{\mathrm{u}}_I(0) = w^{\mathrm{s}}_I(0),$$

so

$$\pi_{X,P_X}\frac{d}{dI}\gamma(I) = \pi_{X,P_X}\frac{d}{dI} w^{\mathrm{u}}_I(0) = \pi_{X,P_X}\frac{d}{dI} w^{\mathrm{s}}_I(0). \tag{76}$$

We now see that from (71), (73–76) we have (5–6).

We now turn to proving (7–8). For a fixed I let us take $x = x_0(\mathcal{X})$ where $\mathcal{X}$ is such that $H_0(L_{\mathcal{X}}) = I$. Let us also consider a fixed $\lambda \in \mathbb{T}$. We see that the unstable and stable fibres of the point $(x, \lambda) \in \Lambda_0$ are parameterised by u and s, respectively, as

$$W^u_{(x,\lambda)} = \left\{\left(\pi_{X,P_X} w^{\mathrm{u}}_I(u), I, \theta^{\mathrm{u}}_{I,\lambda}(u)\right) : u \in \mathbb{R}\right\},$$
$$W^s_{(x,\lambda)} = \left\{\left(\pi_{X,P_X} w^{\mathrm{s}}_I(s), I, \theta^{\mathrm{s}}_{I,\lambda}(s)\right) :\ s \in \mathbb{R}\right\},$$

where $\theta^{\mathrm{u}}_{I,\lambda}, \theta^{\mathrm{s}}_{I,\lambda} : \mathbb{R} \to \mathbb{T}$ are some functions, which parameterise the fibers along the angle coordinate. Hence for every I, θ

$$T_{(\gamma(I),\theta)} W^u_{(x,\theta)} = \operatorname{span}\left\{\left(\pi_{X,P_X}\frac{d}{du} w^{\mathrm{u}}_I(u)|_{u=0}, 0, \frac{d}{du}\theta^{\mathrm{u}}_{I,\theta}(u)|_{u=0}\right)\right\}, \tag{77}$$

$$T_{(\gamma(I),\theta)} W^s_{(x,\theta)} = \operatorname{span}\left\{\left(\pi_{X,P_X}\frac{d}{ds} w^{\mathrm{s}}_I(s)|_{s=0}, 0, \frac{d}{ds}\theta^{\mathrm{s}}_{I,\theta}(s)|_{s=0}\right)\right\}. \tag{78}$$

From (74), (75), (76) and (78) we obtain (7). Similarly, from (73), (75), (76) and (77) we have (8). We have thus shown that Γ is a well defined homoclinic channel.

We now discuss the scattering map (70) associated with Γ. For fibers $W^u_{(x_-,\theta_-)}$ and $W^s_{(x_+,\theta_+)}$ to intersect we must have $x_+ = x_-$, since if this was not the case then the points x_-, x_+ would lie on different energy levels, and their fibres would not meet. This means that

$$\sigma(x, \lambda) = (x, \pi_\theta \sigma(x, \lambda)),$$

We now show how to obtain estimates for $\pi_\theta \sigma(x, \lambda)$.

For every $(x, \lambda) \in \Lambda_0$ we have the homoclinic orbit established in section 4.4 (see in particular Table 2) with the initial point $x_0 = x_0(x, \lambda)$ lying on the unstable fiber established in Lemma 35. From (44) it follows that

$$|\pi_\theta x_0(x, \lambda) - \lambda| \le Mr = 3 \cdot 3 \cdot 10^{-8}.$$

As the point $x_0(x,\lambda)$ is iterated by f_0 the angle θ changes. From Remark 40 we know that after the full excursion along the homoclinic from Table 2 we return to the neighbourhood of Λ_0 at an angle $\pi_\theta x_0(x,\lambda) + 42 \cdot h$, where $h = h(x)$ is from the interval (47). Such homoclinic excursion takes five iterates of f_0 (see Table 2) so

$$\pi_\theta f_0^5(x_0(x,\lambda)) = \pi_\theta x_0(x,\lambda) + 42 \cdot h.$$

We know that $f_0^5(x_0(x,\lambda))$ lies in the stable fiber of $f_0^5(\sigma(x,\lambda))$. We also know that

$$f_0^5(\sigma(x,\lambda)) = f_0^5(x, \pi_\theta\sigma(x,\lambda)) = (x, \pi_\theta\sigma(x,\lambda) + 5T(x)),$$

where $T(x)$ is the period of the Lyapunov orbit. From Lemma 35 and the $\mathcal{R}$-symmetry of the system since $f_0^5(x_0(x,\lambda)) \in W^s_{f_0^5(\sigma(x,\lambda))}$ we have

$$\left|\pi_\theta\left(f_0^5(x_0(x,\lambda)) - f_0^5(\sigma(x,\lambda))\right)\right| \leq Mr.$$

This allows us to obtain the following estimate for the scattering map

$$\begin{aligned}
\pi_\theta\sigma(x,\lambda) &= \pi_\theta\sigma(x,\lambda) + 5T(x) - 5T(x) \\
&= \pi_\theta f_0^5(\sigma(x,\lambda)) - 5T(x) \\
&= \pi_\theta f_0^5(x_0(x,\lambda)) + \pi_\theta\left(f_0^5(\sigma(x,\lambda)) - f_0^5(x_0(x,\lambda))\right) - 5T(x) \\
&\in \pi_\theta x_0(x,\lambda) + 42 \cdot h + [-Mr, Mr] - 5T(x) \\
&= \lambda + (\pi_\theta x_0(x,\lambda) - \lambda) + 42 \cdot h + [-Mr, Mr] - 5T(x) \\
&\in \lambda + [-Mr, Mr] + 42 \cdot h + [-Mr, Mr] - 5T(x) \\
&\in \lambda + [-0.82506903038, -0.82506533656]. \qquad (79)
\end{aligned}$$

We have thus obtained our bound for the scattering map of the unperturbed system.

We have finished our discussion about the unperturbed system. Now we turn to showing that for sufficiently small $\varepsilon > 0$ the manifold Λ_0 persists.

Recall the notation $\tilde{\Lambda}_L$ from (53), which stands for our family of Lyapunov orbits in the extended phase space. Recall also that $\Lambda_0 = \tilde{\Lambda}_L \cap \{Y = 0\}$. By Corollary 44 we know that for sufficiently small ε the normally hyperbolic invariant manifold $\tilde{\Lambda}_L$ is perturbed to a nearby manifold $\tilde{\Lambda}_L^\varepsilon$. We thus obtain $\Lambda_\varepsilon := \tilde{\Lambda}_L^\varepsilon \cap \{Y = 0\}$ as the perturbation of Λ_0. Since by Theorem 42 we know that $\tilde{\Lambda}_L^\varepsilon$ is a manifold with a boundary that consists of two, two dimensional invariant KAM tori. These two tori intersected with $\{Y = 0\}$ produce two curves, which are invariant under f_ε. They become boundaries of Λ_ε. Thus Λ_ε is a normally hyperbolic invariant manifold, with boundary, for f_ε. Similarly, all the two dimensional KAM tori in $\tilde{\Lambda}_L^\varepsilon$ become one dimensional invariant tori in Λ_ε.

We now turn to validating the assumptions of Theorem 11 to obtain our result. This will be done in the local coordinates given by the affine change involving $\tilde{A}_0$ and x^*, in which our f_ε is expressed. Recall that in Lemma 30 and Corollary 31 we have established bounds on the intersection of the local unstable manifold of a Lyapunov orbit with $\{Y = 0\}$. This bound is valid in the following neighbourhood of Λ_0

$$U = [-r, r]^4 \times \mathbb{T}, \qquad (80)$$

where $r = 3 \cdot 10^{-8}$ is the constant from Lemma 30. We have performed a computer assisted validation that the constant L_g from (14) is

$$L_g = 90943. \tag{81}$$

This value was computed using the method described in detail in Appendix C. The value obtained in (81) is a large overestimate. By performing more careful checks, for instance by subdividing U into small fragments, the bound can be significantly improved. Due to the small size of the neighbourhood (80) in which we consider the local unstable manifold, we see that the constant C from (15) can is very small:

$$C = r = 3 \cdot 10^{-8}. \tag{82}$$

Thus the large value of L_g is not a problem for us, since L_g enters condition (17) multiplied by C. We use the bound $\bar{m}$ from Remark 34 to compute

$$\lambda = (\bar{m})^{-30} = \frac{1}{1525.16}.$$

The power 30 comes from the fact that to complete a full turn round a Lyapunov orbit involves 30 local maps (29); see Table 1. We consider the following strips[5]

$$\begin{aligned} S^- &= \Lambda_0 \cap \{\theta \in [0.65 - 0.125, 0.65 + 0.125]\}, \\ S^+ &= \Lambda_0 \cap \{\theta \in [\pi + 0.65 - 0.125, \pi + 0.65 + 0.125]\}. \end{aligned}$$

For each point $z \in S^+$ we compute $m = m(z)$ such that condition (16) is fulfilled. Depending on the choice of z the resulting m can differ. To compute it we used the bound on σ from (79) and the fact that the inner dynamics is given by (69) with the bound on $T(\mathcal{X})$ from (27). We check the assumptions of Theorem 9 by subdividing S^+ into 25 fragments along the θ coordinate, and validated the assumptions for each fragment independently. For the first three fragments for which θ was closest to $\pi + 0.65 - 0.125$ it turned out that a good choice is $m(z) = 21$; for three fragments with θ close to $\pi + 0.65 + 0.125$ we used $m(z) = 25$; and for the remaining we took $m(z) = 23$. For $z \in S^+$ the point $x \in W^u_z$ from condition 2. from Theorem 9, is taken as the first point from homoclinic orbit from Lemma 37. For the alignment of x along θ we use the estimate (44) from Lemma 35. We then validate that

$$\sum_{i=0}^{m(z)-1} \pi_I g\left(0, f_0^i(x)\right) - \frac{1+\lambda}{1-\lambda} L_g C > 0. \tag{83}$$

The inequality (83) is validated with the aid of computer assisted estimates.

In the similar fashion we validate the assumptions of Theorem 10.

Conditions 1. and 2. from Theorem 11 are simple to validate since for every point $z = (x_0(\mathcal{X}), \lambda) \in \Lambda_0$ we have

$$\pi_\theta f(z) = \lambda + T(\mathcal{X}),$$

where $T(\mathcal{X})$ is the period of the Lyapunov orbit, whose bound is known to us in (27). ■

[5]The positioning of the strips was motivated by computing $\sum_{i=0}^{4} \pi_I g\left(0, f_0^i(x)\right)$, which represents the change of energy after the homoclinic excursion along the homoclinic. These five terms in the sum play the leading role in (83). In Figure 4 we provide a plot of computer assisted bounds on $\sum_{i=0}^{4} \pi_I g\left(0, f_0^i(x)\right)$, for different choices of $\pi_\theta z$, and place our strips S^+, S^- for reference in the figure.

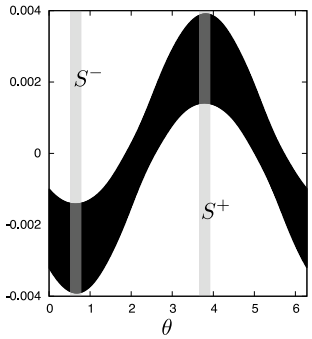

Figure 4: The computer assisted bound for the first five terms in the sum in (83), depending on $\pi_\theta z$.

Remark 46. *Due to the fact that we work with the particular family of Lyapunov orbits, which correspond to the energy of the comet Oterma, it turned out that the m used in conditions 1. and 2. from Theorems 9 and 10 was a large number. This resulted in the need of large number of iterates of f_0 when computing (83), which meant long integration time. Also, we needed relatively wide strips S^+, S^-. This meant that we needed many subdivisions of the strips to perform our validation. The long integration time and the large number of sets increased the computational time of our proof. By making a more careful choice of the energy level, one could focus on Lyapunov orbits for which m would be smaller. We have chosen not to do so to demonstrate that the method is applicable for the choice of energy dictated by a concrete physical object.*

Appendix A. Proof of Lemma 27

Proof. Take $v \in Q^+(0) \cap B$. Since $a_i \in (0,1)$ we see that $|v_1| \geq |v_i| / a_{i-1} > |v_i|$, for $i = 2,3,4$. Since $f(0) = 0$ from the mean value theorem we obtain

$$\begin{aligned}
\|f(v)\|_{\max} &= \|f(v) - f(0)\|_{\max} \\
&\in \left\| [Df(B)]\, v \right\|_{\max} \\
&= \|(A_{11}v_1 + A_{12}(v_2,v_3,v_4), A_{21}v_1 + A_{22}(v_2,v_3,v_4))\|_{\max} \\
&\geq |A_{11}v_1 + A_{12}(v_2,v_3,v_4)| \\
&\geq (c - \|A_{12}\|_{\max} \max(a_1,a_2,a_3)) |v_1| \\
&= (c - \|A_{12}\|_{\max} \max(a_1,a_2,a_3)) \|v\|_{\max},
\end{aligned}$$

as required. ■

Appendix B. Proof of Lemma 28

Proof. Let $v = (v_1, v_2)$ where $v_1 = \pi_1 v$ and $v_2 = \pi_{2,3,4} v$. Since $v \in Q^+(0)$ we see that

$$|v_1| \geq a^{-1} \|v_2\|_{\max}.$$

From the mean value theorem we obtain

$$\begin{aligned}\|f(v)\|_{\max} &\in \left\|\left[Df(B)\right]v\right\|_{\max}\\ &= \|(A_{11}v_1 + A_{12}v_2, A_{21}v_1 + A_{22}v_2)\|_{\max}\\ &\leq \max\left(|A_{11}|\,|v_1| + \|A_{12}\|_{\max}\|v_2\|_{\max}, \|A_{21}\|_{\max}|v_1| + \|A_{22}\|_{\max}\|v_2\|_{\max}\right)\\ &\leq \max\left(|A_{11}| + a\|A_{12}\|_{\max}, \|A_{21}\|_{\max} + a\|A_{22}\|_{\max}\right)|v_1|\\ &= \max\left(|A_{11}| + a\|A_{12}\|_{\max}, \|A_{21}\|_{\max} + a\|A_{22}\|_{\max}\right)\|v\|_{\max}\end{aligned}$$

as required. ■

Appendix C. Lipschitz bounds for the perturbation term

Here we give a method, with which we can check (14) in the case when $I(x)$ is defined as (65). Below we start with Lemma 47, that can be applied to achieve this. We have found though that in our particular case of the PER3BP, due to long integration times, a direct application of Lemma 47 leads to overestimates, which were too large for our needs. We therefore follow with Lemma 48, which can be used for an inductive computation of L_g by expressing f_ε as a composition of maps. This allowed us to avoid long integration times and improved the estimate.

Lemma 47. *Let $D^2I(x)$ stand for the Hessian of I at x. Consider $x_0, x_1 \in \mathbb{R}^3\times\mathbb{S}$ and let $\mathbf{x} \subset \mathbb{R}^3\times\mathbb{S}$ be a convex set which contains x_0 and x_1. Let $\mathbf{v} \subset \mathbb{R}^4$ be the following interval enclosure*

$$\mathbf{v}^\top = \left[\left(\frac{\partial f_0}{\partial\varepsilon}(\mathbf{x})\right)^\top D^2I(f_0(\mathbf{x}))\,Df_0(\mathbf{x}) + DI(f_0(\mathbf{x}))\,\frac{\partial^2 f_0}{\partial x\partial\varepsilon}(\mathbf{x})\right].$$

If $\|\mathbf{v}\| \leq L_g$ then

$$|\pi_I g(0,x_1) - \pi_I g(0,x_0)| \leq L_g\|x_1 - x_0\|.$$

Proof. Let

$$x_s := x_0 + s(x_1 - x_0).$$

From (68) we obtain

$$\begin{aligned}&\pi_I g(0,x_1) - \pi_I g(0,x_0)\\ &= \int_0^1 \frac{d}{ds}\nabla I(f_0(x_s))\cdot\frac{\partial f_0}{\partial\varepsilon}(x_s)\,ds\\ &= \int_0^1 D^2I(f_0(x_s))\,Df_0(x_s)(x_1 - x_0)\cdot\frac{\partial f_0}{\partial\varepsilon}(x_s) + \nabla I(f_0(x_s))\cdot\frac{\partial^2 f_0}{\partial x\partial\varepsilon}(x_s)(x_1 - x_0)\,ds\\ &= \int_0^1 \frac{\partial f_0}{\partial\varepsilon}(x_s)\cdot D^2I(f_0(x_s))\,Df_0(x_s)(x_1 - x_0) + \nabla I(f_0(x_s))\cdot\frac{\partial^2 f_0}{\partial x\partial\varepsilon}(x_s)(x_1 - x_0)\,ds\\ &= \left(\int_0^1 \left(\frac{\partial f_0}{\partial\varepsilon}(x_s)\right)^\top D^2I(f_0(x_s))\,Df_0(x_s) + DI(f_0(x_s))\,\frac{\partial^2 f_0}{\partial x\partial\varepsilon}(x_s)\,ds\right)(x_1 - x_0)\\ &\in \mathbf{v}\cdot(x_1 - x_0),\end{aligned}$$

so

$$|\pi_I g(0,x_1) - \pi_I g(0,x_0)| \leq \|\mathbf{v}\|\,\|x_1 - x_0\| \leq L_g\|x_1 - x_0\|,$$

as required. ■

We now consider the case where f is a composition of two functions $f = f_\varepsilon^1 \circ f_\varepsilon^2$. Our objective will be to compute Lipschitz bound in terms of x for

$$g(\varepsilon, x) := \frac{1}{\varepsilon}\left(I \circ f_\varepsilon^2 \circ f_\varepsilon^1(\varepsilon, x) - I(x)\right). \tag{C.1}$$

The following lemma gives the bound for $\pi_I g(0, x)$ from bounds for f_ε^1 and f_ε^2.

Lemma 48. *Assume that*

$$\begin{aligned} f_\varepsilon &= f_\varepsilon^2 \circ f_\varepsilon^1, \\ g(\varepsilon, x) &= \frac{1}{\varepsilon}\left(f_\varepsilon(x) - f_0(x)\right), \\ g_1(\varepsilon, x) &= \frac{1}{\varepsilon}\left(f_\varepsilon^1(x) - f_0^1(x)\right), \\ g_2(\varepsilon, x) &= \frac{1}{\varepsilon}\left(f_\varepsilon^2(x) - f_0^2(x)\right), \end{aligned}$$

and that

$$\begin{aligned} \|\pi_I(g_1(0, x_1) - g_1(0, x_0))\| &\le L_g^1 \|x_1 - x_0\|, \\ \|\pi_I(g_2(0, x_1) - g_2(0, x_0))\| &\le L_g^2 \|x_1 - x_0\|, \\ \left\|f_0^1(x_1) - f_0^1(x_0)\right\| &\le L_f^1 \|x_1 - x_0\|. \end{aligned}$$

Then

$$\|\pi_I(g(0, x_1) - g(0, x_0))\| \le \left(L_g^2 L_f^1 + L_g^1\right)\|x_1 - x_0\|.$$

Proof. Consider fixed x_1, x_0. Then

$$\begin{aligned} &\|\pi_I g(\varepsilon, x_1) - \pi_I g(\varepsilon, x_0)\| \\ &= \left\|\frac{1}{\varepsilon}\left(I \circ f_\varepsilon^2 \circ f_\varepsilon^1(x_1) - I(x_1) - \left(I \circ f_\varepsilon^2 \circ f_\varepsilon^1(x_0) - I(x_0)\right)\right)\right\| \\ &\le \left\|\frac{1}{\varepsilon}\left(I \circ f_\varepsilon^2 \circ f_\varepsilon^1(x_1) - I \circ f_\varepsilon^1(x_1) - \left(I \circ f_\varepsilon^2 \circ f_\varepsilon^1(x_0) - I \circ f_\varepsilon^1(x_0)\right)\right)\right\| \\ &\quad + \left\|\frac{1}{\varepsilon}\left(I \circ f_\varepsilon^1(x_1) - I(x_1) - \left(I \circ f_\varepsilon^1(x_0) - I(x_0)\right)\right)\right\| \\ &= \left\|\pi_I g_2\left(\varepsilon, f_\varepsilon^1(x_1)\right) - \pi_I g_2\left(\varepsilon, f_\varepsilon^1(x_0)\right)\right\| + \|\pi_I g_1(\varepsilon, x_1) - \pi_I g_1(\varepsilon, x_0)\| \\ &\le L_g^2 \left\|f_\varepsilon^1(x_1) + f_\varepsilon^1(x_0)\right\| + L_g^1 \|x_1 + x_0\| + o(\varepsilon) \\ &\le \left(L_g^2 L_f^1 + L_g^1\right)\|x_1 + x_0\| + o(\varepsilon) \end{aligned}$$

and the result follows by passing with ε to zero. ■

The bound (14) computed in the proof (see section 4.6) is for the Poincaré map f_ε defined in (64). This can be computed by considering

$$f_\varepsilon = f_{\varepsilon,N} \circ \ldots \circ f_{\varepsilon,1}, \tag{C.2}$$

where $f_{\varepsilon,i}$ are local maps of the form

$$f_{\varepsilon,i}(x) = A_i^{-1}\left(\Phi_t^{\varepsilon}(x_{i-1} + A_{i-1}x) - x_i\right) \qquad \text{for } i = 1, \dots, N-1,$$
$$f_{\varepsilon,N}(x) = A_0^{-1}\left(\mathcal{P}^{\varepsilon}(x_{N-1} + A_{N-1}x) - x_0\right).$$

In the inductive application of Lemma 48 we can use the bound $\bar{m}$ from Remark 34 and take $L_f^1 = \bar{m}^k$ at the k-th inductive step.

The energy after an iterate of a local map is

$$I\left(f_{\varepsilon,i}(x)\right) = H_0\left(\Phi_t^{\varepsilon}(x_{i-1} + A_{i-1}x)\right).$$

Since

$$\begin{aligned}
&\frac{d}{dx}\frac{d}{d\varepsilon}H_0\left(\Phi_t^{\varepsilon}(x_{i-1} + A_{i-1}x)\right)\\
&= \frac{d}{dx}\left(\nabla H_0\left(\Phi_t^{\varepsilon}(x_{i-1} + A_{i-1}x)\right) \cdot \frac{\partial \Phi_t^{\varepsilon}}{\partial \varepsilon}(x_{i-1} + A_{i-1}x)\right)\\
&= \left(\frac{\partial \Phi_t^{\varepsilon}}{\partial \varepsilon}(x_{i-1} + A_{i-1}x)\right)^{\top} D^2 H_0\left(\Phi_t^{\varepsilon}(x_{i-1} + A_{i-1}x)\right)\frac{\partial \Phi_t^{\varepsilon}}{\partial x}(x_{i-1} + A_{i-1}x)\,A_{i-1}\\
&\quad + DH_0\left(\Phi_t^{\varepsilon}(x_{i-1} + A_{i-1}x)\right)\frac{\partial^2 \Phi_t^{\varepsilon}}{\partial x \partial \varepsilon}(x_{i-1} + A_{i-1}x)\,A_{i-1}
\end{aligned}$$

the $\mathbf{v}^{\top}$ used for the computation of L_g for a local map $f_{\varepsilon,i}$ by means of Lemma 47 is computed as

$$\mathbf{v}^{\top} = \left[\left(\frac{\partial \Phi_t^{\varepsilon}}{\partial \varepsilon}(\mathbf{x})\right)^{\top} D^2 H_0\left(\Phi_t^{\varepsilon}(\mathbf{x})\right)\frac{\partial \Phi_t^{\varepsilon}}{\partial x}(\mathbf{x})\,A_{i-1} + DH_0\left(\Phi_t^{\varepsilon}(\mathbf{x})\right)\frac{\partial^2 \Phi_t^{\varepsilon}}{\partial x \partial \varepsilon}(\mathbf{x})\,A_{i-1}\right]. \tag{C.3}$$

(For the last local map $f_{\varepsilon,N}$ we take $\mathcal{P}^{\varepsilon}$ instead of Φ_t^{ε} in (C.3).)

References

[1] V. I. Arnol'd, Instability of dynamical systems with many degrees of freedom, Dokl. Akad. Nauk SSSR 156 (1964) 9–12.

[2] A. Delshams, R. de la Llave, T. M. Seara, Geometric properties of the scattering map of a normally hyperbolic invariant manifold, Adv. Math. 217 (3) (2008) 1096–1153.
URL https://doi-org.ezproxy.fau.edu/10.1016/j.aim.2007.08.014

[3] A. Delshams, R. Ramírez-Ros, Poincaré-Mel'nikov-Arnol'd method for analytic planar maps, Nonlinearity 9 (1) (1996) 1–26. doi:10.1088/0951-7715/9/1/001.
URL https://doi.org/10.1088/0951-7715/9/1/001

[4] M. Gidea, R. de la Llave, T. M-Seara, A general mechanism of diffusion in Hamiltonian systems: qualitative results, Comm. Pure Appl. Math. 73 (1) (2020) 150–209. doi:10.1002/cpa.21856.
URL https://doi.org/10.1002/cpa.21856

[5] M. Gidea, R. de la Llave, T. M. Seara, A general mechanism of instability in Hamiltonian systems: skipping along a normally hyperbolic invariant manifold, Discrete Contin. Dyn. Syst. 40 (12) (2020) 6795–6813. doi:10.3934/dcds.2020166.
URL https://doi.org/10.3934/dcds.2020166

[6] M. J. Capiński, J. Gonzalez, J.-P. Marco, J. D. Mireles James, Computer assisted proof of drift orbits along normally hyperbolic manifolds, https://arxiv.org/abs/2102.06436.
URL https://arxiv.org/abs/2102.06436

[7] A. Delshams, V. Kaloshin, A. de la Rosa, T. M. Seara, Global instability in the restricted planar elliptic three body problem, Comm. Math. Phys. 366 (3) (2019) 1173–1228. doi:10.1007/s00220-018-3248-z.
URL https://doi.org/10.1007/s00220-018-3248-z

[8] M. J. Capiński, M. Gidea, Arnold diffusion, quantitative estimates and stochastic behavior in the three-body problem (2020).
URL https://arxiv.org/abs/1812.03665

[9] M. J. Capiński, P. Zgliczyński, Transition tori in the planar restricted elliptic three-body problem, Nonlinearity 24 (5) (2011) 1395–1432. doi:10.1088/0951-7715/24/5/002.
URL https://doi.org/10.1088/0951-7715/24/5/002

[10] M. J. Capiński, M. Gidea, R. de la Llave, Arnold diffusion in the planar elliptic restricted three-body problem: mechanism and numerical verification, Nonlinearity 30 (1) (2017) 329–360. doi:10.1088/1361-6544/30/1/329.
URL https://doi.org/10.1088/1361-6544/30/1/329

[11] T. Kapela, M. Mrozek, D. Wilczak, P. Zgliczyński, Capd::dynsys: a flexible c++ toolbox for rigorous numerical analysis of dynamical systems, Communications in Nonlinear Science and Numerical Simulation (2020) 105578doi:https://doi.org/10.1016/j.cnsns.2020.105578.
URL https://www.sciencedirect.com/science/article/pii/S1007570420304081

[12] G. Alefeld, Inclusion methods for systems of nonlinear equations—the interval Newton method and modifications, in: Topics in validated computations (Oldenburg, 1993), Vol. 5 of Stud. Comput. Math., North-Holland, Amsterdam, 1994, pp. 7–26.

[13] M. W. Hirsch, C. C. Pugh, M. Shub, Invariant manifolds, Bull. Amer. Math. Soc. 76 (1970) 1015–1019. doi:10.1090/S0002-9904-1970-12537-X.
URL https://doi.org/10.1090/S0002-9904-1970-12537-X

[14] V. Szebehely, Theory of Orbits: The Restricted Problem of Three Bodies, Academic Press, 1967.

[15] W. S. Koon, M. W. Lo, J. E. Marsden, S. D. Ross, Heteroclinic connections between periodic orbits and resonance transitions in celestial mechanics, Chaos 10 (2) (2000) 427–469. doi:10.1063/1.166509.
URL https://doi.org/10.1063/1.166509

[16] M. J. Capiński, Computer assisted existence proofs of Lyapunov orbits at L_2 and transversal intersections of invariant manifolds in the Jupiter-Sun PCR3BP, SIAM J. Appl. Dyn. Syst. 11 (4) (2012) 1723–1753. doi:10.1137/110847366.
URL https://doi.org/10.1137/110847366